Electronic Supplementary Information

Modulating proton conductivity through crystal structure tuning in arenedisulfonate coordination polymers

Chao Sun,[a,b] Christopher M. Pask,[b] Sang The Pham,[a,b,c] Emilio Rapaccioli,[b] Andrew J. Britton,[a,c] Stuart Micklethwaite,[a,c] Andrew Bell,[a] Maximilian O. Besenhard,[d] Rik Drummond-Brydson,[a,c] Ke-Jun Wu,[a,e] Sean M. Collins,[a,b,c*]

a. School of Chemical and Process Engineering, University of Leeds, Leeds LS2 9JT, UK
b. School of Chemistry, University of Leeds, Leeds LS2 9JT, UK
c. Bragg Centre for Materials Research, University of Leeds, Leeds LS2 9JT, UK
d. Department of Chemical Engineering, University College London, London WC1E 7JE, UK
e. Zhejiang Provincial Key Laboratory of Advanced Chemical Engineering Manufacture Technology, College of Chemical and Biological Engineering, Zhejiang University, Hangzhou, 310027, China

[*]Email: S.M.Collins@leeds.ac.uk

Figure S1. Digital photograph of the pellet sample testing cell with two plate electrodes.

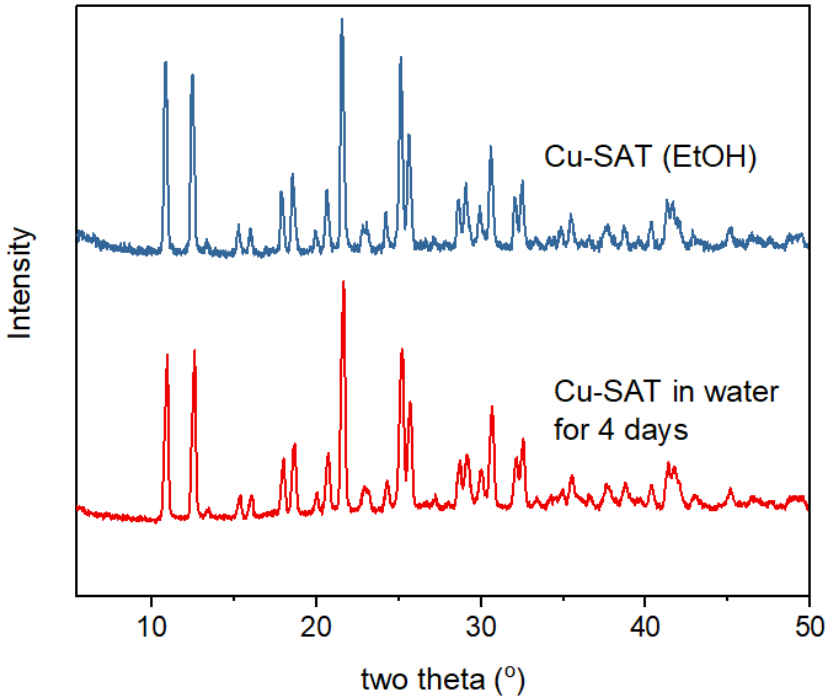

Figure S2. Powder XRD patterns of Cu-SAT after water degradation and the as-synthesized product of Cu-SAT (EtOH).

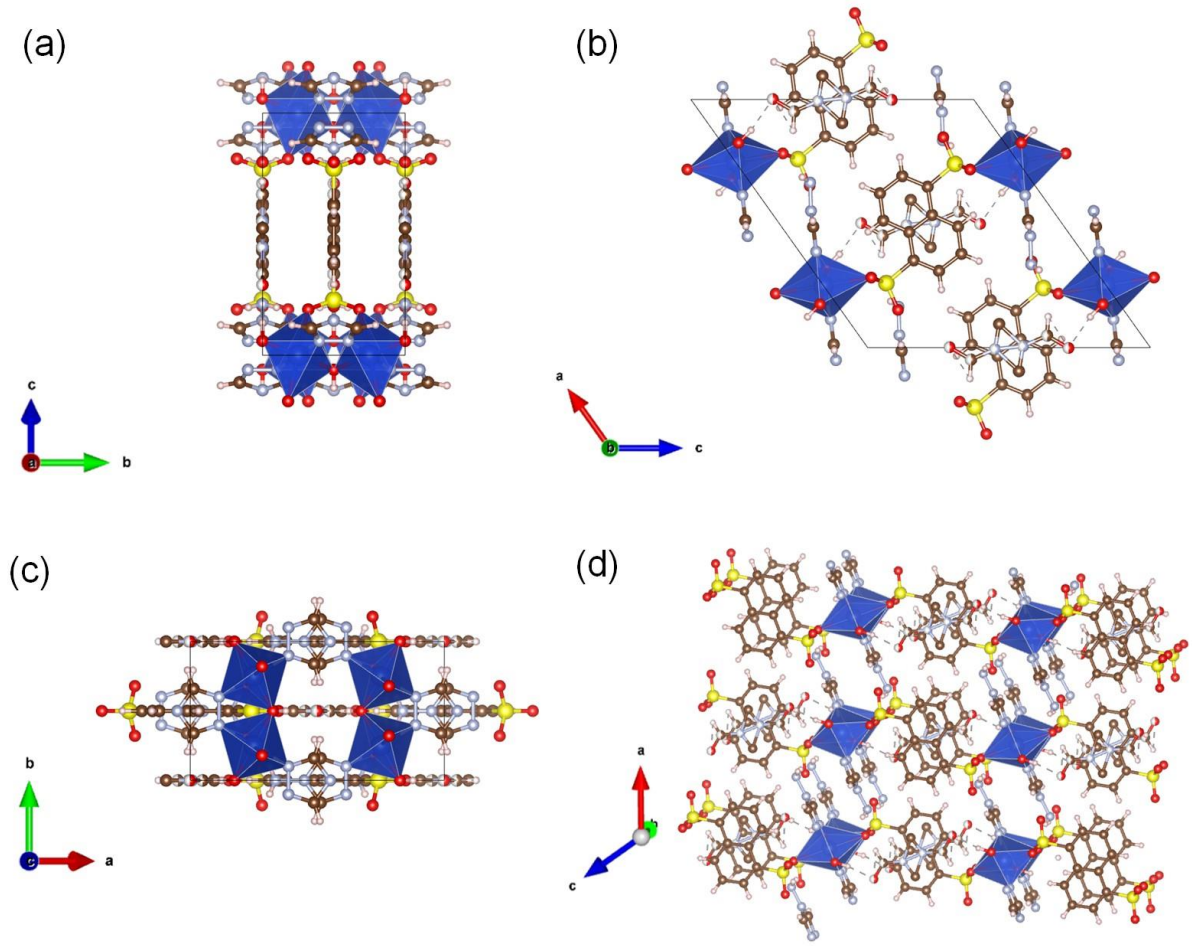

Figure S3. Polyhedral representations of the Cu-SAT unit cell determined by SC-XRD. The unit cell is depicted along (a) the *a*-axis, (b) the *b*-axis, (c) the *c*-axis, and (d) along a direction highlighting the stacked 2D layers formed by the NDS coordination of a Cu^{2+} chain. Atoms are color-coded by element: S, yellow; Cu, blue; O, red; N, light blue; C, brown; H, beige.

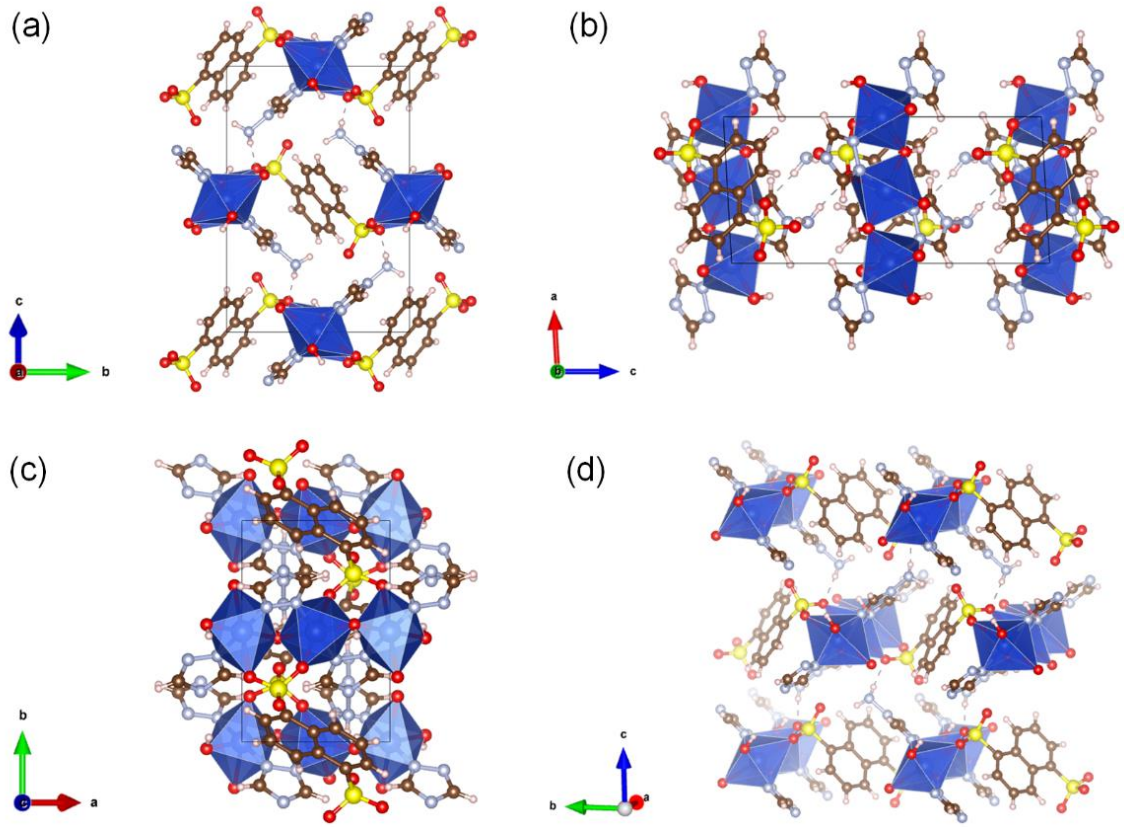

Figure S4. Polyhedral representations of the Cu-SAT (EtOH) unit cell as determined from SC-XRD. The unit cell is depicted along (a) the *a*-axis, (b) the *b*-axis, (c) the *c*-axis, and (d) along a direction highlighting the stacked 2D layers formed by NDS ligand coordination of a Cu^{2+} chain. Atoms are color-coded by element: S, yellow; Cu, blue; O, red; N, light blue; C, brown; H, beige.

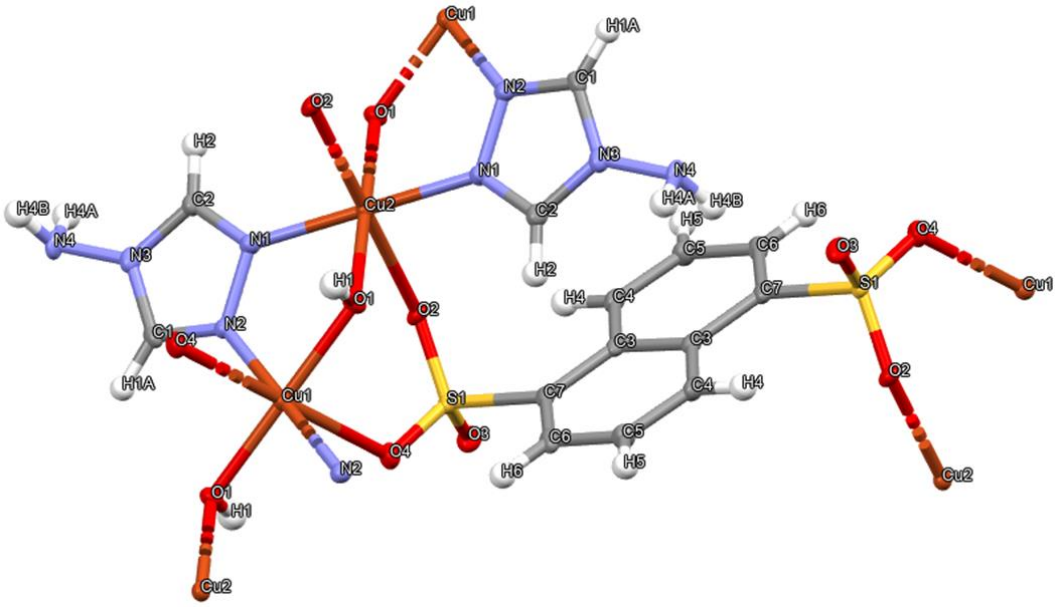

Figure S5. Visualisation of the atomic displacement parameters for the reported Cu-SAT (EtOH) structure showing the determined atoms depicted as ellipsoids (hydrogen atoms shown as spheres for reference).

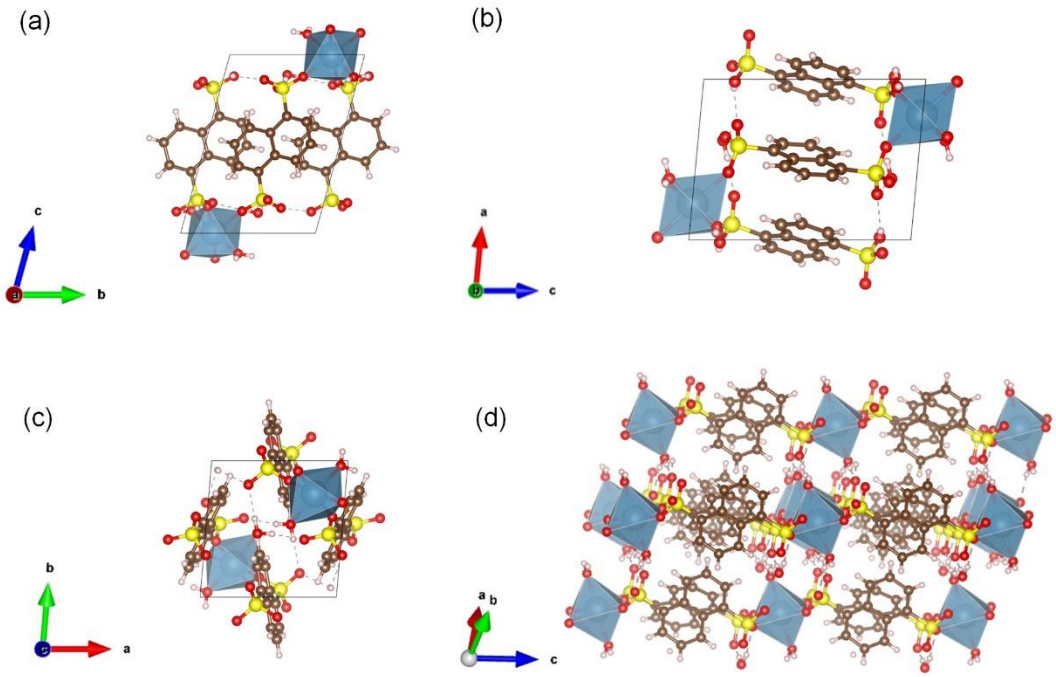

Figure S6. Polyhedral representations of the Ca-NDS (water) unit cell as determined from SC-XRD. The unit cell is depicted along (a) the *a*-axis, (b) the *b*-axis, (c) the *c*-axis, and (d) a direction highlighting the stacked 2D sheet structure formed by the NDS coordination of Ca^{2+}. Atoms are color-coded by element: S, yellow; Ca, dusty blue; O, red; C, brown; H, beige.

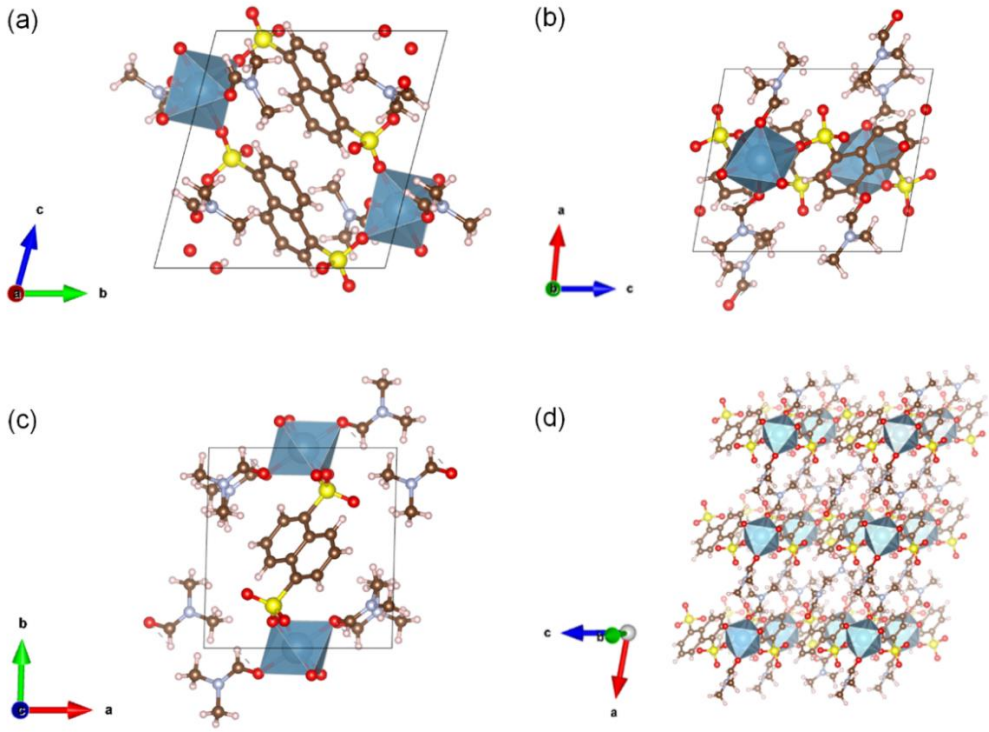

Figure S7. Polyhedral representations of the Ca-NDS (DMF) unit cell as determined from SC-XRD. The unit cell is depicted along (a) the *a*-axis, (b) the *b*-axis, (c) the *c*-axis, and (d) a direction highlighting the stacked 2D sheet structure formed by the NDS coordination of Ca^{2+}. Atoms are color-coded by element: S, yellow; Ca, dusty blue; O, red; C, brown; N, light blue; H, beige.

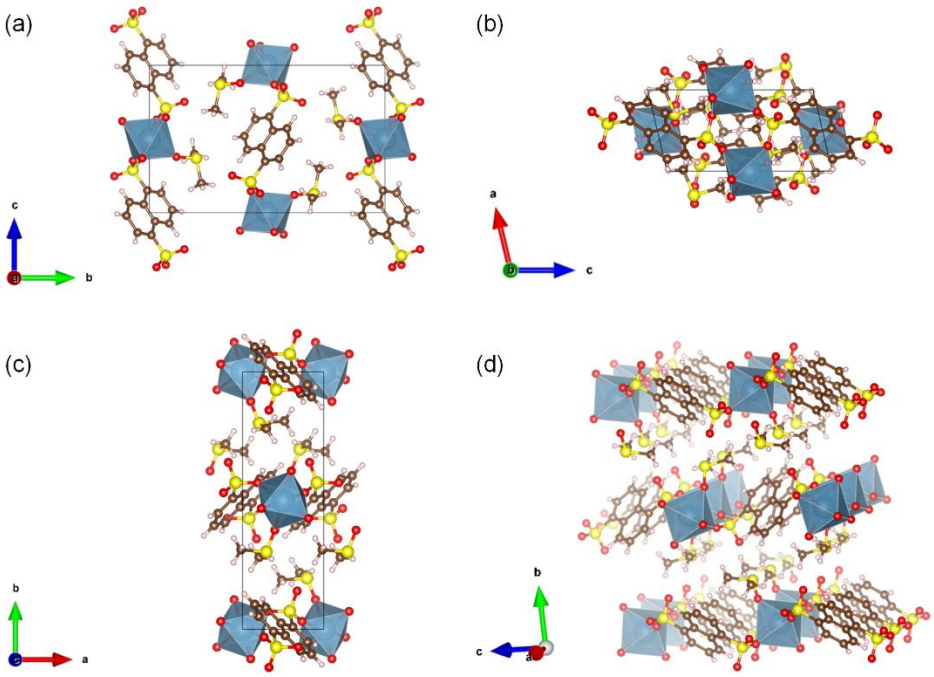

Figure S8. Polyhedral representations of the Ca-NDS (DMSO) structure as determined from SC-XRD. The unit cell is depicted along (a) the *a*-axis, (b) the *b*-axis, (c) the *c*-axis, and (d) a direction highlighting the stacked 2D sheet structure formed by NDS coordination of Ca^{2+}. Atoms are color-coded by element: S, yellow; Ca, dusty blue; O, red; C, brown; H, beige.

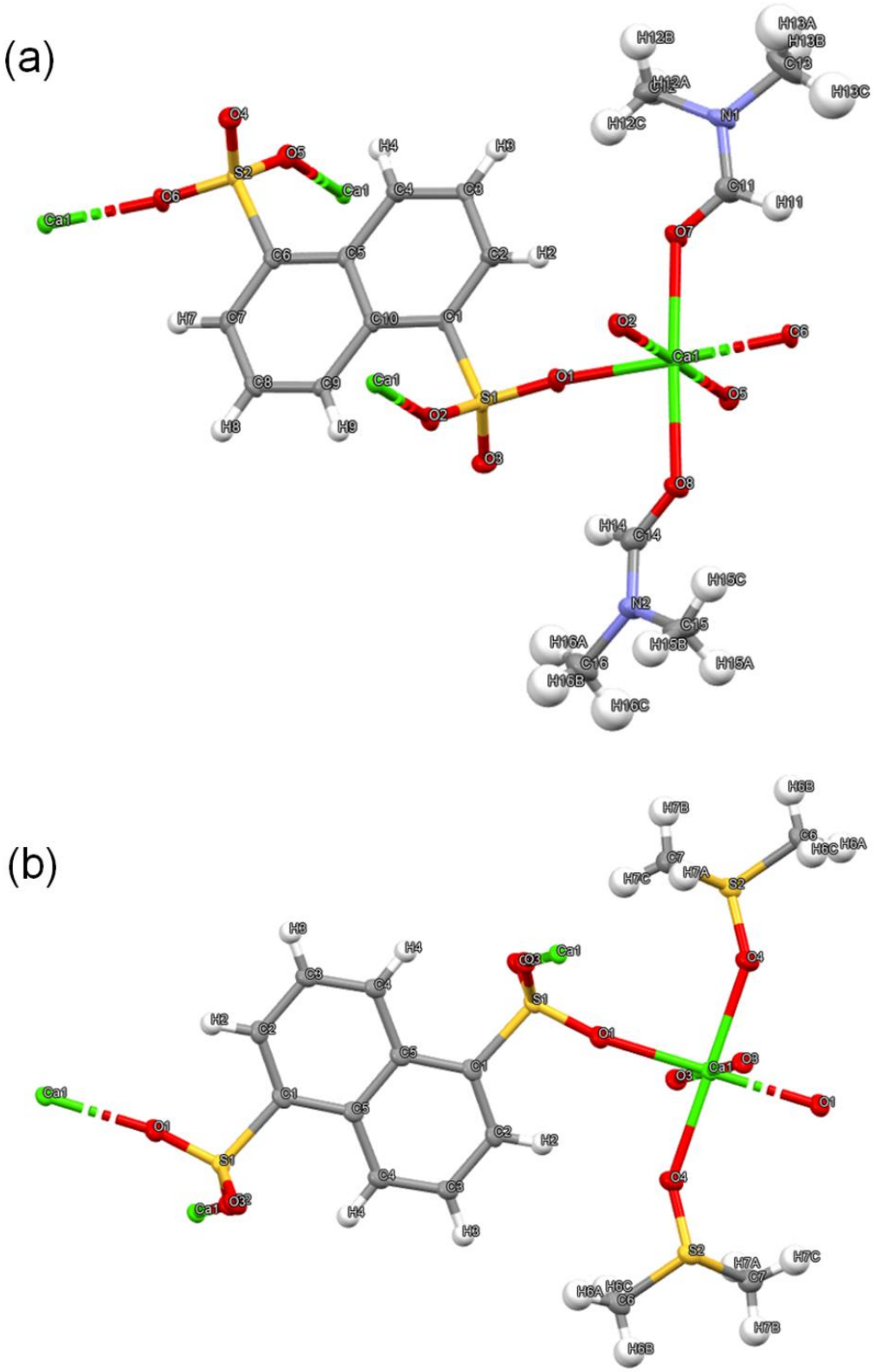

Figure S9. Visualisations of the atomic displacement parameters (a) for the reported Ca-NDS (DMF) structure and (b) for the reported Ca-NDS (DMSO) structure. The visualisations show the determined atoms depicted as ellipsoids (hydrogen atoms shown as spheres for reference).

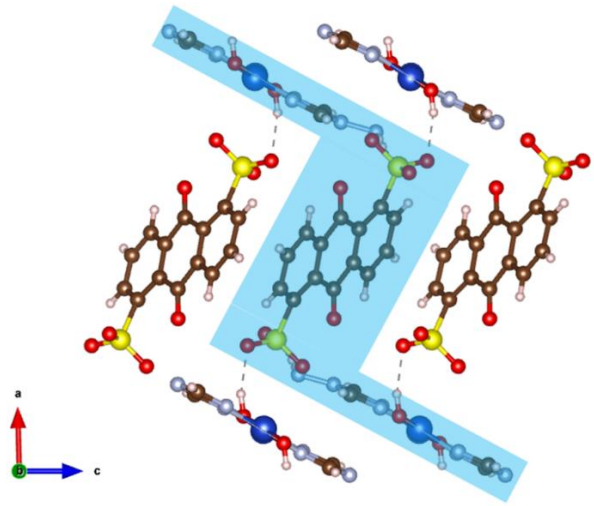

Figure S10. Polyhedral representation of Cu-SQAT depicting a side-on view along the crystallographic *b*-axis (the shading highlights 3D coordination between layers). Atoms are color-coded by element: S, yellow; Cu, blue; O, red; N, light blue; C, brown; H, beige.

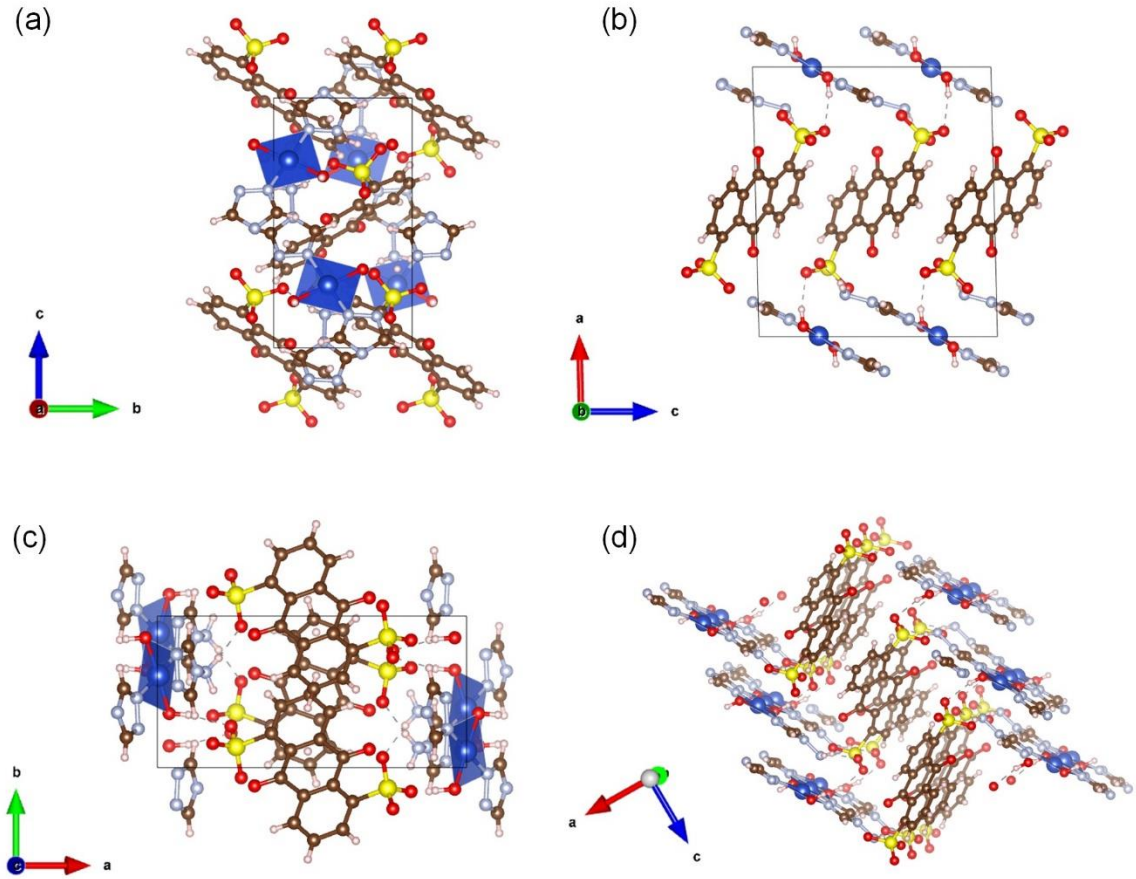

Figure S11. Polyhedral representations of the Cu-SQAT unit cell as determined from SC-XRD. The unit cell is depicted along (a) the *a*-axis, (b) the *b*-axis, (c) the *c*-axis, and (d) a direction highlighting the corrugated 2D sheet structure formed by the ADS coordination of the Cu^{2+} chain. Atoms are color-coded by element: S, yellow; Cu, blue; O, red; N, light blue; C, brown; H, beige.

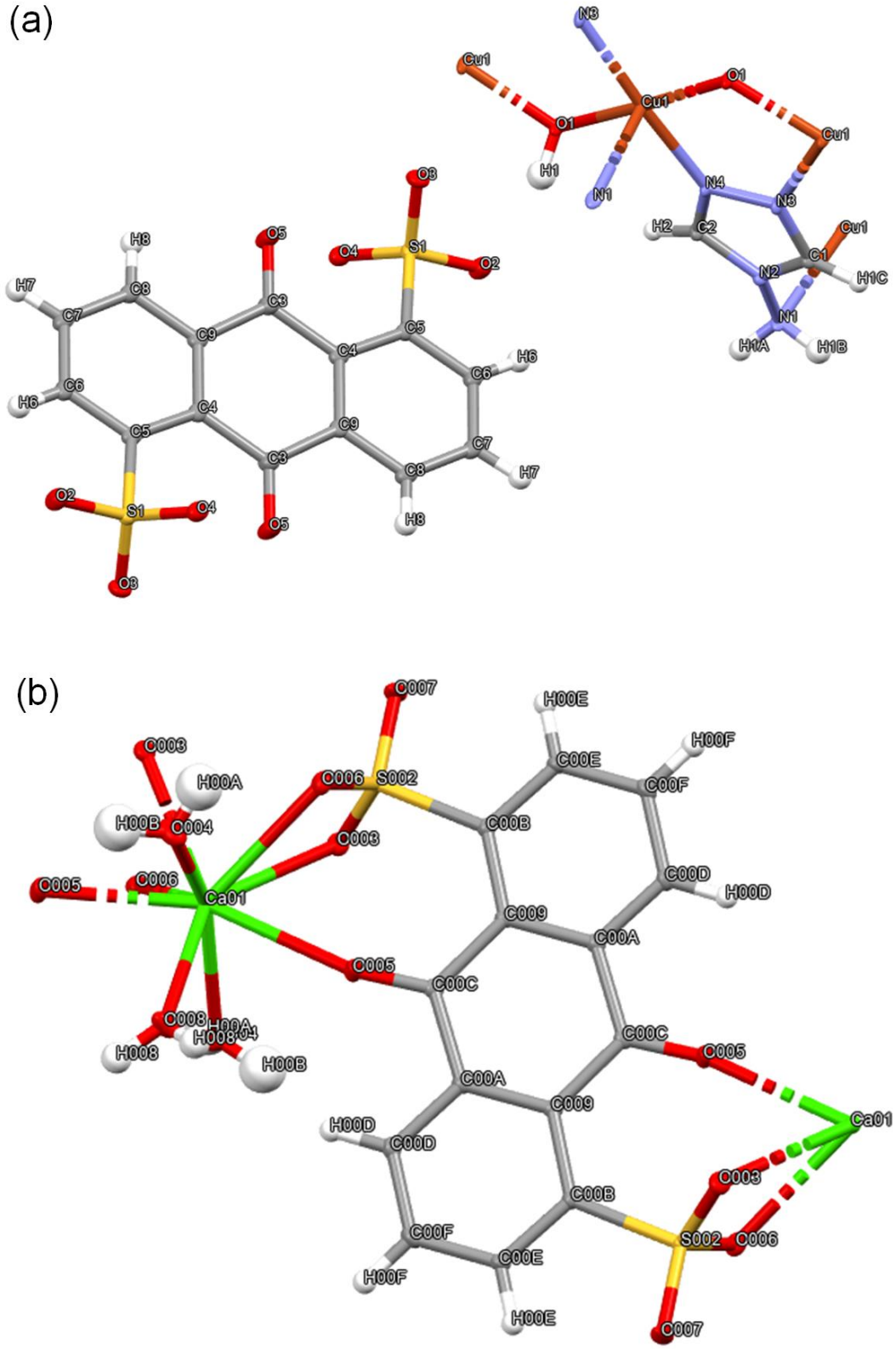

Figure S12. Visualisations of the atomic displacement parameters (a) for the reported Cu-SQAT structure and (b) for the reported Ca-ADS structure. The visualisations show the determined atoms depicted as ellipsoids (hydrogen atoms shown as spheres for reference).

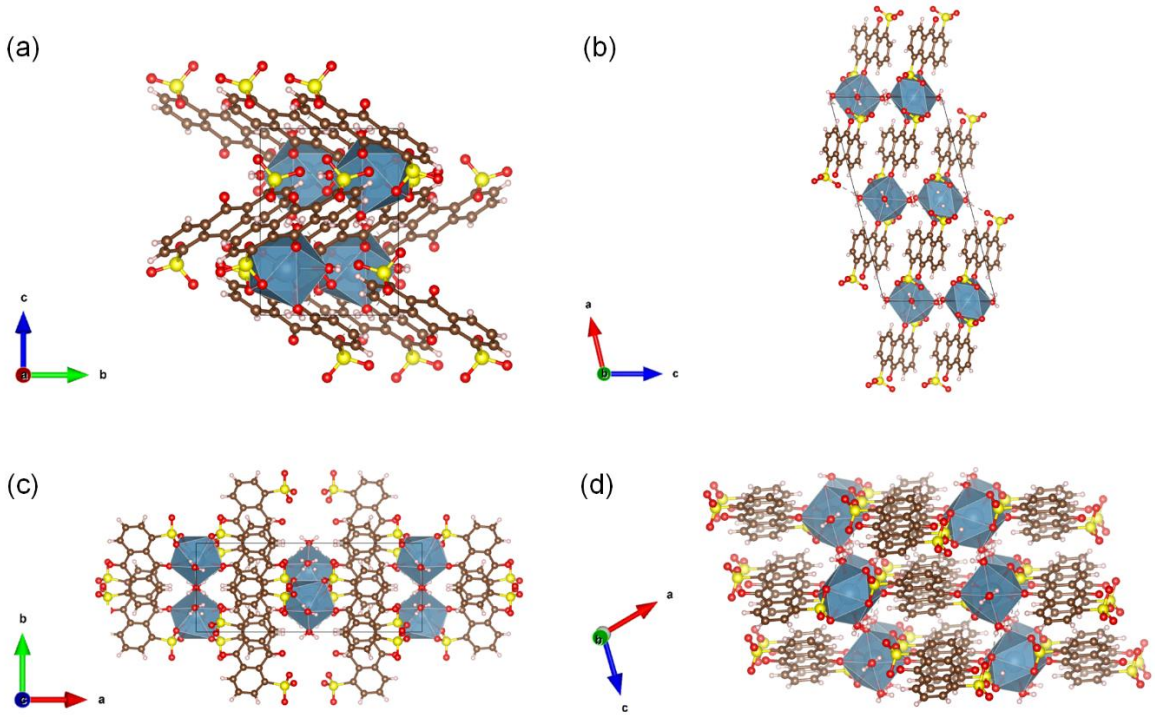

Figure S13. Polyhedral representations of the Ca-ADS unit cell as determined from SC-XRD. The unit cell is depicted along (a) the *a*-axis, (b) the *b*-axis, (c) the *c*-axis, and (d) a direction highlighting the stacked 2D sheet structure arising from ADS coordination of Ca^{2+} (2D sheet of 1D chains). Atoms are color-coded by element: S, yellow; Ca, dusty blue; O, red; C, brown; H, beige.

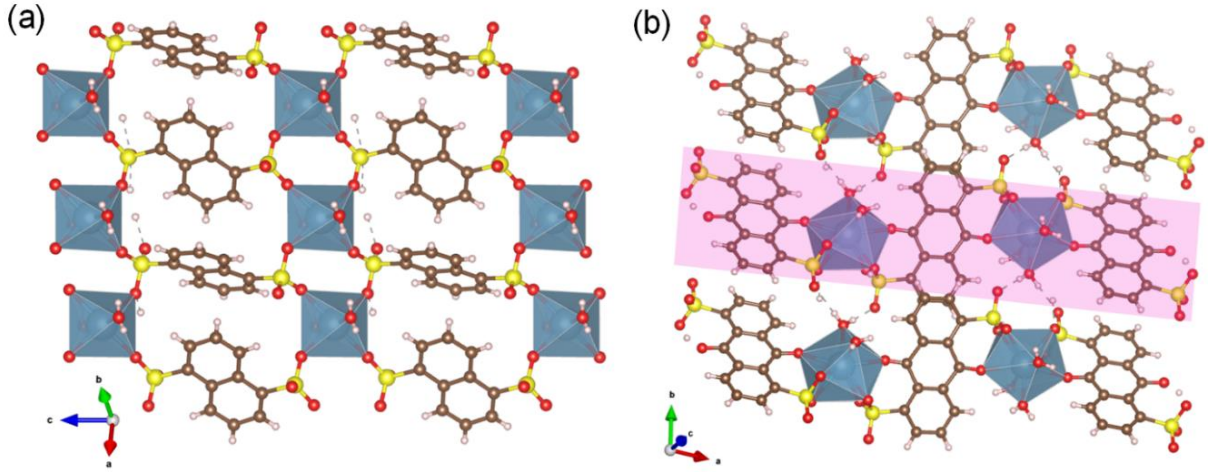

Figure S14. Polyhedral representation of (a) the 2D sheet structure of Ca-NDS (water) and (b) the 1D chain structure of Ca-ADS (the shading highlights the 1D chain). Atoms are color-coded by element: S, yellow; Ca, dusty blue; O, red; C, brown; H, beige.

Table S1. CHNS analysis as molar ratios (H = 1) for Cu-SAT and Cu-SAT (EtOH). The elemental ratios for the Cu-SAT and Cu-SAT (EtOH) unit cells (SC-XRD) are included for comparison. Uncertainties are given as one standard deviation.

Sample	N	C	H	S	Ratio of N to S
Cu-SAT a	0.40	0.85	1.00	0.10	4.00
Cu-SAT b	0.40	0.85	1.00	0.11	3.77
Cu-SAT c	0.38	0.80	1.00	0.11	3.45
AVG results of Cu-SAT	0.39 ± 0.01	0.83 ± 0.03	1.00	0.11 ± 0.01	3.74 ± 0.28
Unit cell formula Cu-SAT	0.52	0.94	1.00	0.12	4.25
Cu-SAT (EtOH) a	0.52	1.01	1.00	0.15	3.45
Cu-SAT (EtOH) b	0.52	1.01	1.00	0.15	3.45
Cu-SAT (EtOH) c	0.47	0.97	1.00	0.14	3.47
AVG results of Cu-SAT (EtOH)	0.50 ± 0.03	0.99 ± 0.02	1.00	0.14 ± 0.01	3.46 ± 0.01
Unit cell formula Cu-SAT (EtOH)	0.50	0.88	1.00	0.13	3.85

Table S2. CHNS analysis as molar ratios (H = 1) for Ca-NDS (water), Ca-NDS (DMF) and Ca-NDS (DMSO). The elemental ratios for the Ca-NDS (DMF) and Ca-NDS (DMSO) unit cells (SC-XRD) are included for comparison. Uncertainties are given as one standard deviation.

Sample	N	C	H	S	Ratio of N to S
Ca-NDS (water) a	0.02	1.15	1.00	0.23	--
Ca-NDS (water) b	0.02	0.87	1.00	0.16	--
Ca-NDS (water) c	0.03	1.10	1.00	0.26	
AVG results of Ca-NDS (water)	0.02 ± 0.01	1.04 ± 0.15	1.00	0.21 ± 0.05	--
Unit cell formula Ca-NDS (water)	--	1.00	1.00	0.20	--
Ca-NDS (DMF) a	0.11	1.10	1.00	0.19	0.08
Ca-NDS (DMF) b	0.09	1.11	1.00	0.19	0.07
Ca-NDS (DMF) c	0.13	1.12	1.00	0.29	0.07
AVG results of Ca-NDS (DMF)	0.11 ± 0.02	1.11 ± 0.01	1.00	0.22 ± 0.06	0.07 ± 0.01
Unit cell formula Ca-NDS (DMF)	0.10	0.80	1.00	0.10	1.00
Ca-NDS (DMSO) a	0.02	1.13	1.00	0.20	--
Ca-NDS (DMSO) b	0.01	0.68	1.00	0.12	--
Ca-NDS (DMSO) c	0.03	1.03	1.00	0.25	
AVG results of Ca-NDS (DMSO)	0.02 ± 0.01	0.94 ± 0.23	1.00	0.19 ± 0.07	--
Unit cell formula Ca-NDS (DMSO)	--	0.78	1.00	0.22	--

Table S3. CHNS analysis as molar ratios (H = 1) for Cu-SQAT and Ca-ADS. The elemental ratios for the Cu-SQAT and Ca-ADS unit cells (SC-XRD) are included for comparison. Uncertainties are given as one standard deviation.

Sample	N	C	H	S	Ratio of N to S
Cu-SQAT a	0.51	1.26	1.00	0.14	3.54
Cu-SQAT b	0.51	1.26	1.00	0.15	3.52
Cu-SQAT c	0.46	1.21	1.00	0.13	3.56
AVG results of Cu-SQAT	0.49 ± 0.03	1.24 ± 0.03	1.00	0.14 ± 0.01	3.54 ± 0.02
Unit cell formula Cu-SQAT	0.50	1.13	1.00	0.13	4.00
Ca-ADS a	0.02	1.20	1.00	0.16	--
Ca-ADS b	0.02	1.07	1.00	0.14	--
Ca-ADS c	0.04	1.29	1.00	0.21	
AVG results of Ca-ADS	0.03 ± 0.01	1.19 ± 0.11	1.00	0.17±0.04	--
Unit cell formula Ca-ADS	--	1.17	1.00	0.17	--

Table S4. Elemental composition of Cu-SAT (EtOH) and Cu-SQAT from SEM-EDS analysis (Atomic %) determined using the Cliff-Lorimer method (manufacturer-supplied k-factors). The elemental ratios for the Cu-SAT (EtOH) and Cu-SQAT unit cells (SC-XRD) are included for comparison.

Sample	C %	O %	N %	S %	Cu %	Ratio of Cu/(Cu+S)
Cu-SAT (EtOH)	46.4	19.7	20.1	6.9	6.3	0.48
Unit cell formula Cu-SAT (EtOH)	41.2	23.5	23.5	5.9	5.9	0.5
Cu-SQAT	49.3	21.0	18.4	5.4	5.9	0.52
Unit cell formula Cu-SQAT	45	25	20	5	5	0.5

Table S5. Elemental composition of Ca-NDS (DMF), Ca-NDS (DMSO) and Ca-ADS from SEM-EDS analysis (Atomic %) determined using the Cliff-Lorimer method (manufacturer-supplied k-factors). The elemental ratios for the Ca-NDS (DMF), Ca-NDS (DMSO) and Ca-ADS unit cells (SC-XRD) are included for comparison.

Sample	C %	O %	N %	S %	Ca %	Ratio of Ca/(Ca+S)
Ca-NDS (DMF)	55.6	28.3	1.9	9.4	4.8	0.34
Unit cell formula Ca-NDS (DMF)	55.2	27.6	6.9	6.9	3.4	0.33
Ca-NDS (DMSO)	59.3	15.0	--	14.3	3.7	0.21
Unit cell formula Ca-NDS (DMSO)	51.9	29.6	--	14.8	3.7	0.2
Ca-ADS	58.0	29.0	--	8.6	4.4	0.34
Unit cell formula Ca-ADS	50	39.3	--	7.1	3.6	0.34

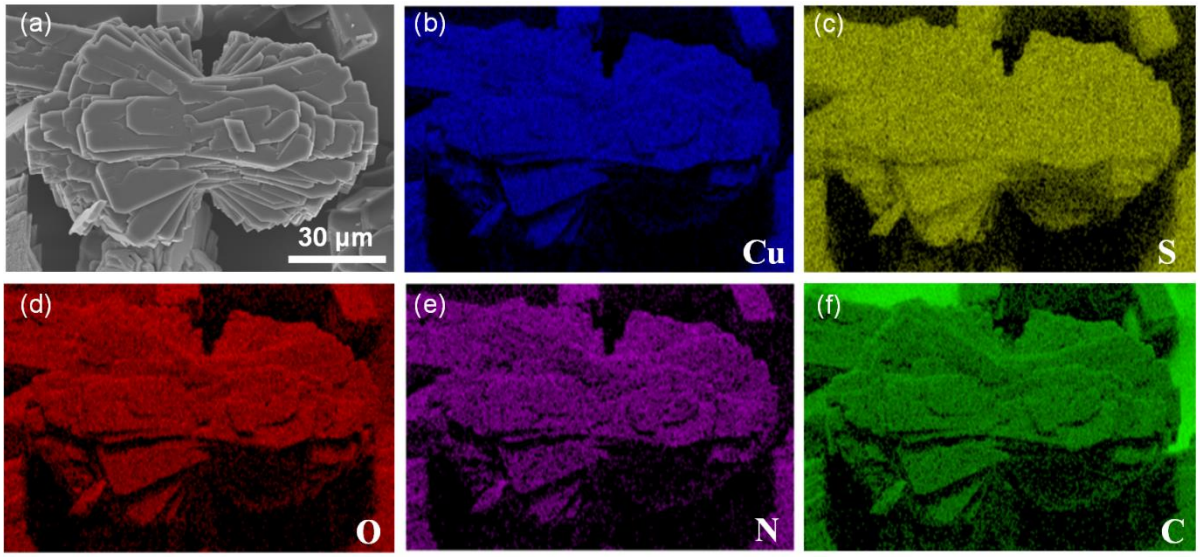

Figure S15. (a) SEM image of a Cu-SAT (EtOH) particle and SEM-EDS elemental maps of (b) copper, (c) sulfur, (d) oxygen, (e) nitrogen, and (f) carbon.

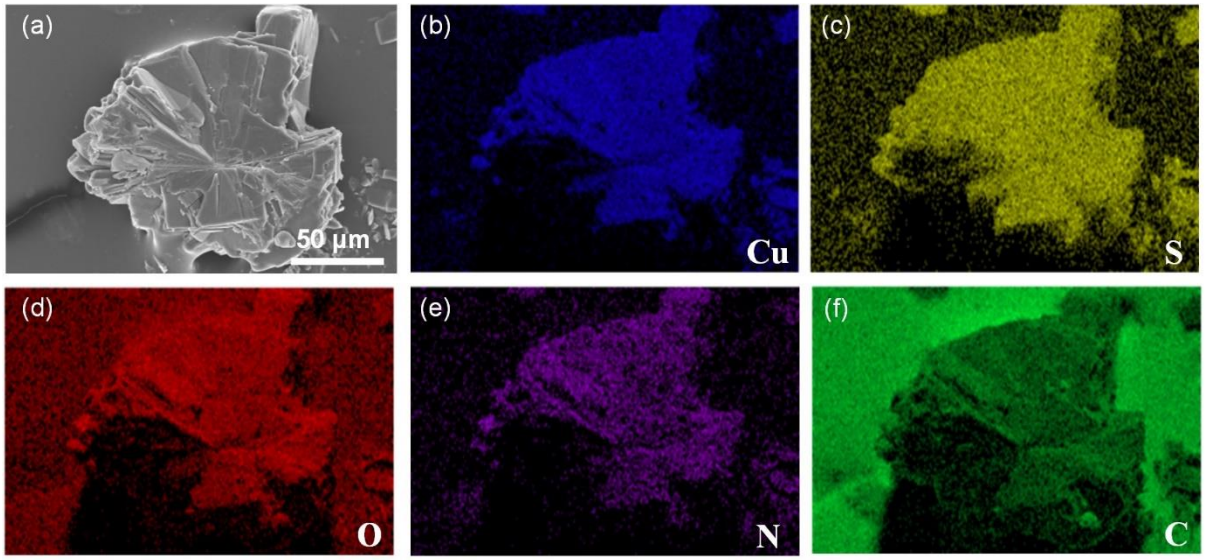

Figure S16. (a) SEM image of a Cu-SQAT particle and SEM-EDS elemental maps of (b) copper, (c) sulfur, (d) oxygen, (e) nitrogen, and (f) carbon.

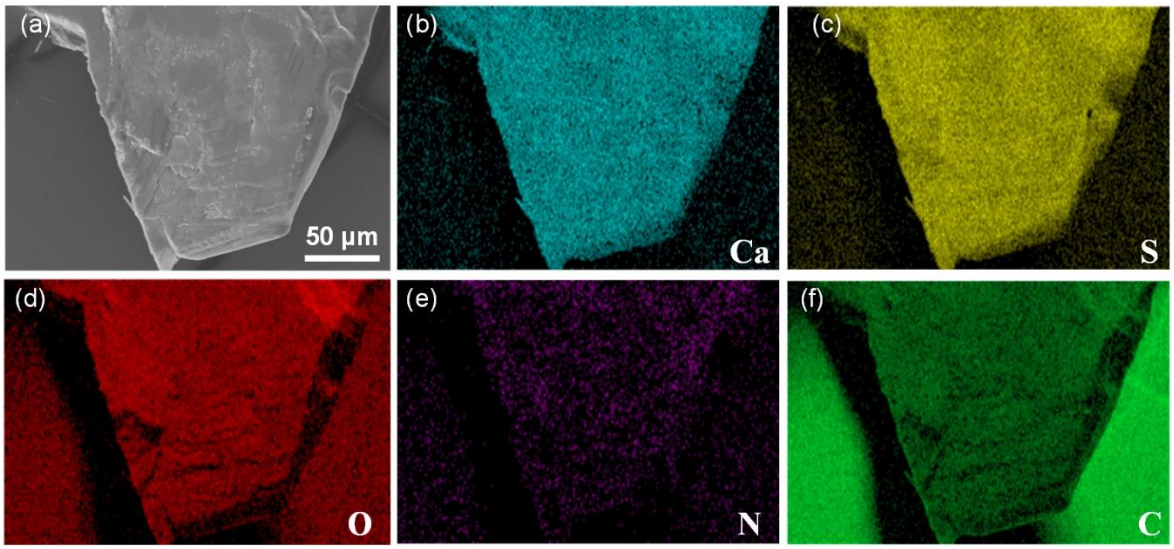

Figure S17. (a) SEM image of a Ca-NDS (DMF) particle and SEM-EDS elemental maps of (b) calcium, (c) sulfur, (d) oxygen, (e) nitrogen, and (f) carbon.

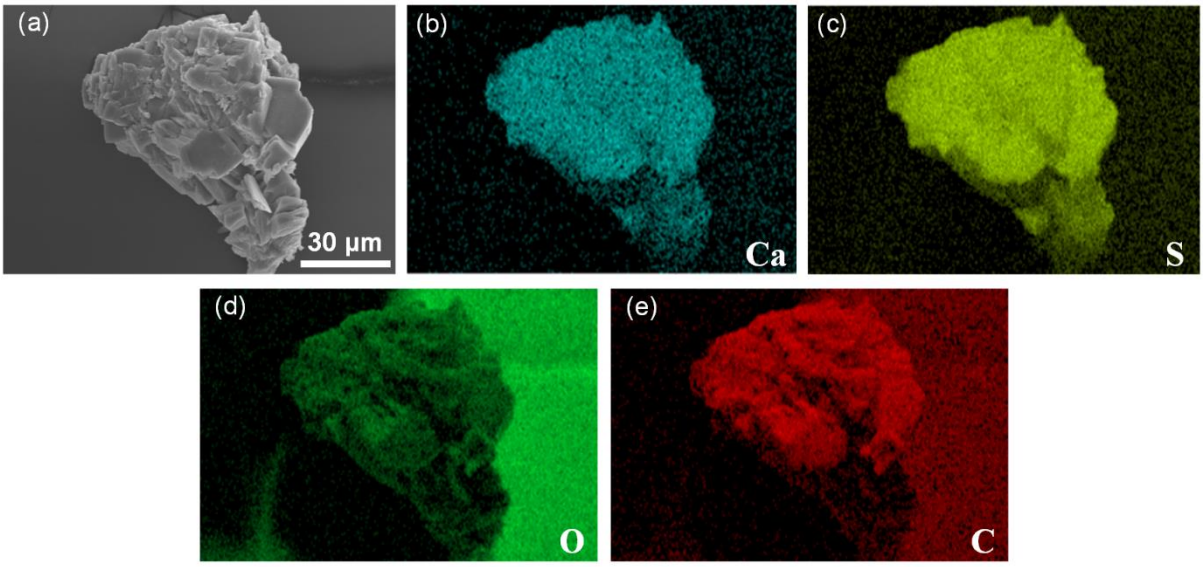

Figure S18. (a) SEM image of a Ca-NDS (DMSO) particle and SEM-EDS elemental maps of (b) calcium, (c) sulfur, (d) oxygen, and (e) carbon.

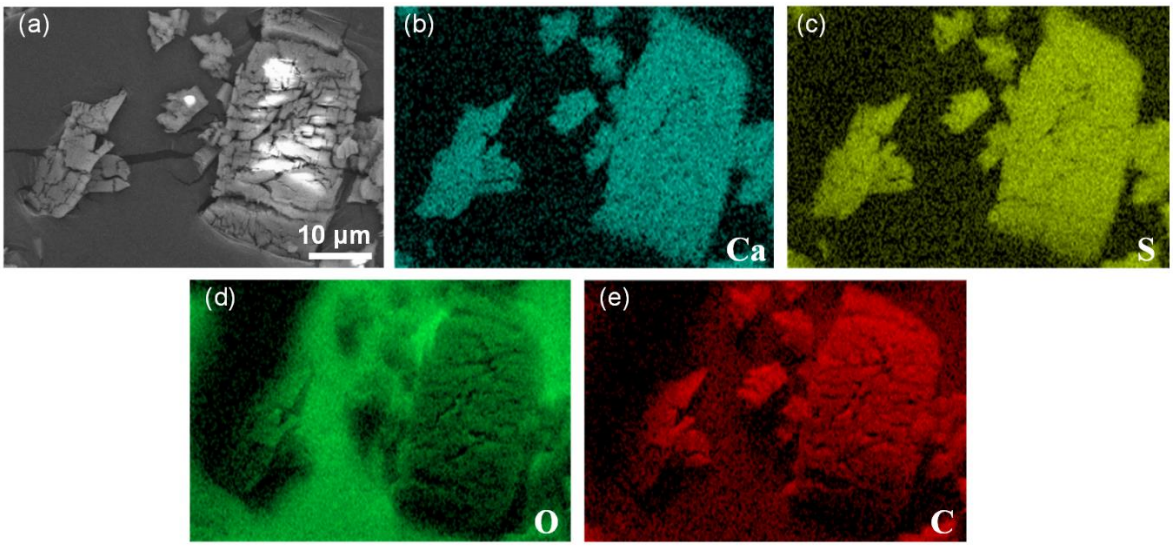

Figure S19. (a) SEM image of a Ca-ADS particle and SEM-EDS elemental maps of (b) calcium, (c) sulfur, (d) oxygen, and (e) carbon.

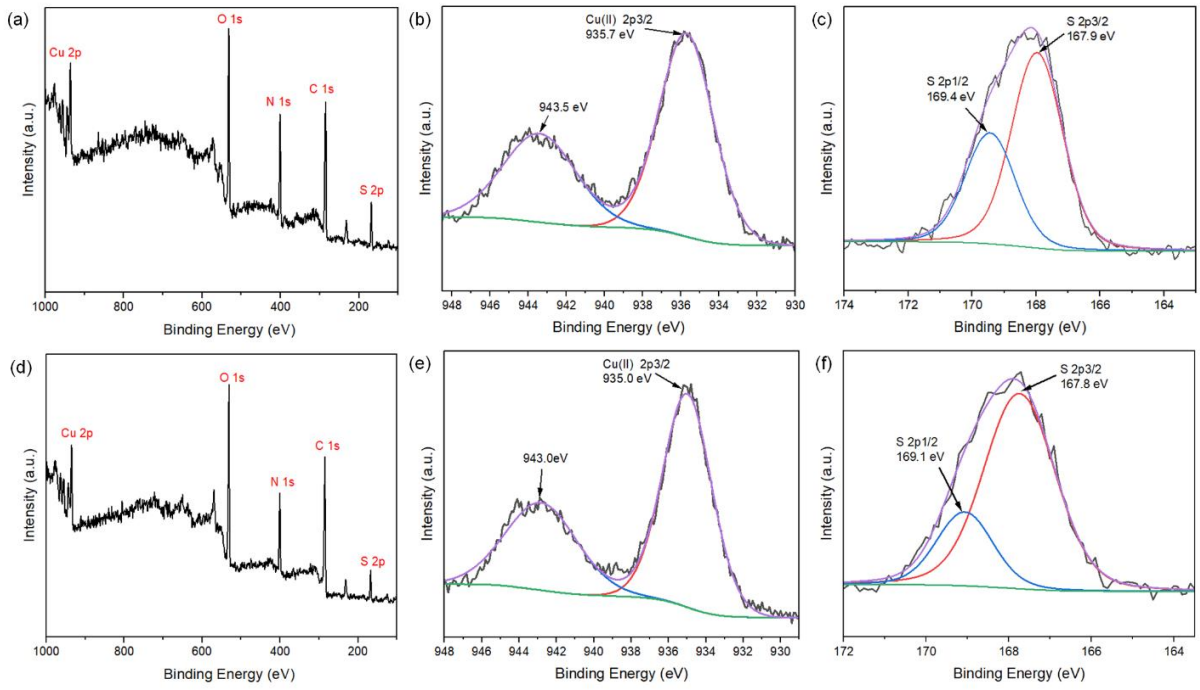

Figure S20. XPS analysis of Cu-SAT (EtOH) and Cu-SQAT, showing (a) survey spectra, (b) high resolution scans of Cu $2p_{3/2}$, and (c) high resolution scans of S $2p_{3/2}$ for Cu-SAT (EtOH), and (d) survey spectra, (e) high resolution scans of Cu $2p_{3/2}$, and (f) high resolution scans of S $2p_{3/2}$ for Cu-SQAT (Ar sputtering carried out prior to analysis).

Table S6 Elemental composition analysis of Cu-SAT (EtOH) and Cu-SQAT by XPS (Ar sputtering before analysis). The elemental ratios for the Cu-SAT (EtOH) and Cu-SQAT unit cells (SC-XRD) are included for comparison.

Sample	C 1s %	O 1s %	N 1s %	S 2p %	Cu 2p %	Ratio of Cu/(Cu+S)
Cu-SAT (EtOH)	52.5	19.6	18.4	5.8	3.7	0.39
Unit cell formula Cu-SAT (EtOH)	41.2	23.5	23.5	5.9	5.9	0.5
Cu-SQAT	51.3	23.0	16.1	5.6	4.0	0.38
Unit cell formula Cu-SQAT	45	25	20	5	5	0.5

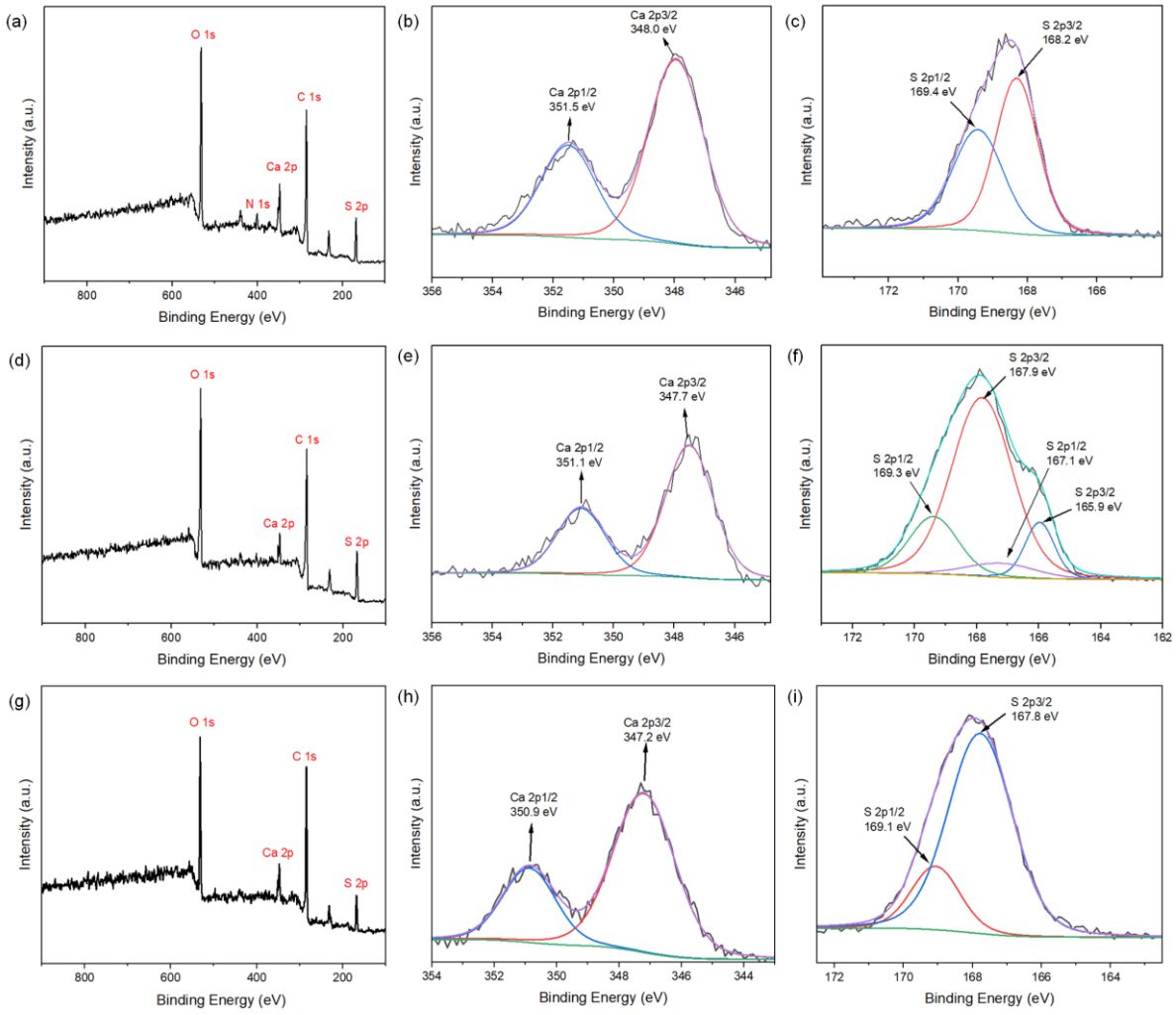

Figure S21. XPS analysis of Ca-NDS (DMF), Ca-NDS (DMSO), and Ca-ADS, showing (a) survey spectra, (b) high resolution scans of Ca $2p_{3/2}$, and (c) high resolution scans of S $2p_{3/2}$ for Ca-NDS (DMF), (d) survey spectra, (e) high resolution scans of Ca $2p_{3/2}$, and (f) high resolution scans of S $2p_{3/2}$ for Ca-NDS (DMSO), and (g) survey spectra, (h) high resolution scans of Ca $2p_{3/2}$, and (i) high resolution scans of S $2p_{3/2}$ for Ca-ADS.

Table S7 Elemental composition of Ca-NDS (DMF), Ca-NDS (DMSO) and Ca-ADS from XPS analysis. The elemental ratios for the Ca-NDS (DMF), Ca-NDS (DMSO) and Ca-ADS unit cells (SC-XRD) are included for comparison.

Sample	C 1s %	O 1s %	N 1s %	S 2p %	Ca 2p %	Ratio of Ca/(Ca+S)
Ca-NDS (DMF)	58	23.4	3.1	10.8	4.7	0.3
Unit cell formula Ca-NDS (DMF)	55.2	27.6	6.9	6.9	3.4	0.33
Ca-NDS (DMSO)	62.4	22.1	--	13.1	2.4	0.15
Unit cell formula Ca-NDS (DMSO)	51.9	29.6	--	14.8	3.7	0.2
Ca-ADS	65	21.8	--	9.8	3.5	0.26
Unit cell formula Ca-ADS	50	39.3	--	7.1	3.6	0.34

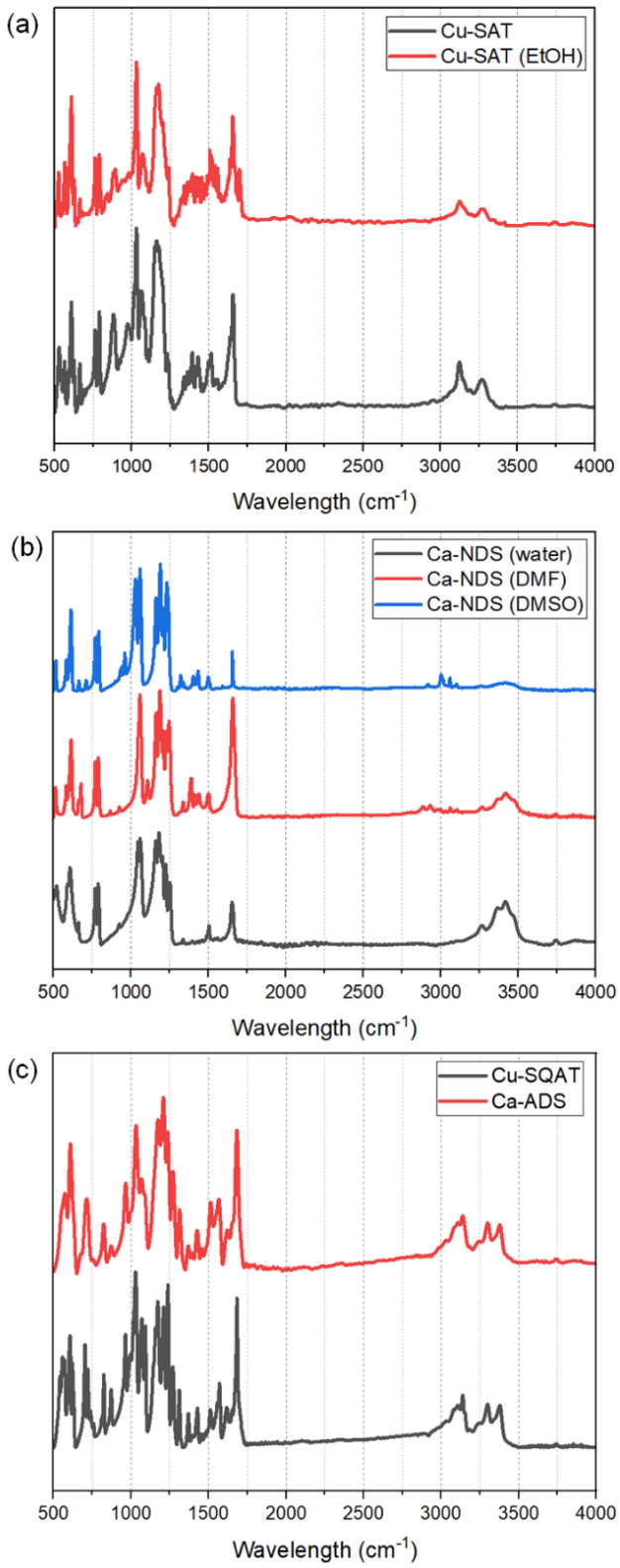

Figure S22. ATR-FTIR spectra of (a) Cu-SAT and Cu-SAT (EtOH), (b) Ca-NDS (water), Ca-NDS (DMF) and Ca-NDS (DMSO), and (c) Cu-SQAT and Ca-ADS samples.

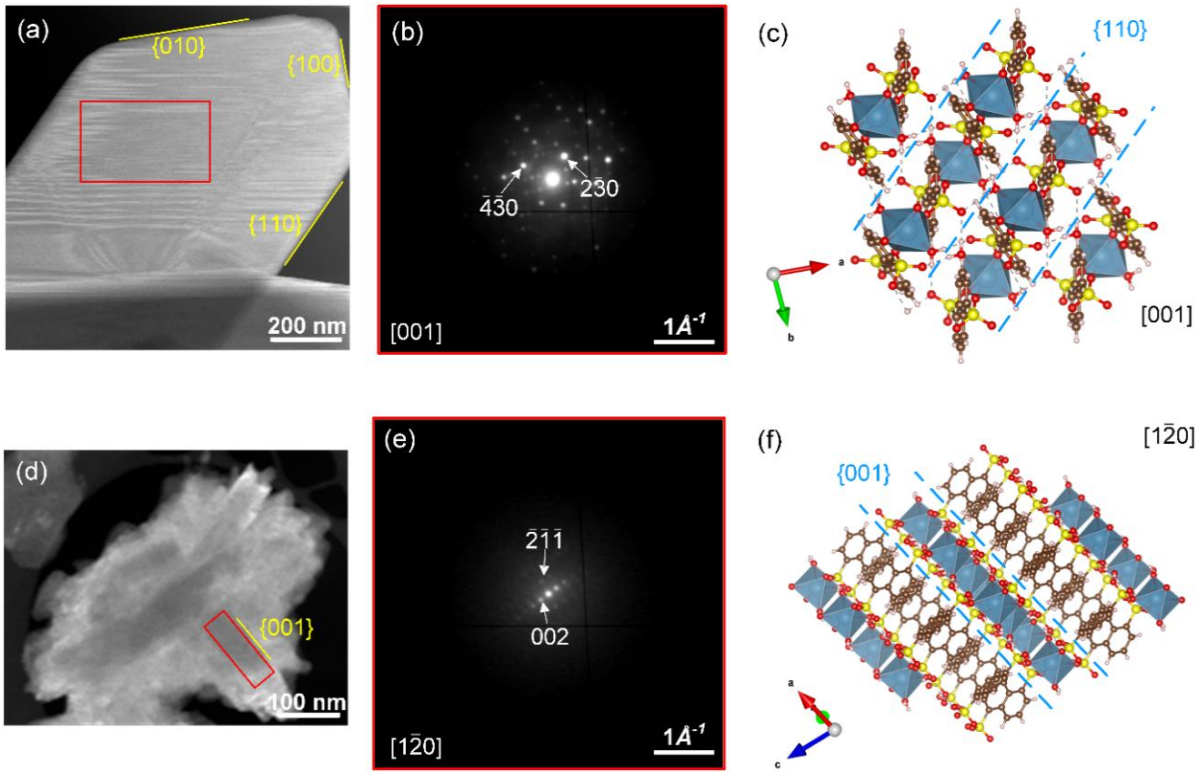

Figure S23. (a) and (d) Annular dark field STEM images of Ca-NDS (water) particles. (b) and (e) Corresponding diffraction patterns extracted from scanning electron diffraction data in the areas marked by the red rectangles. (c) and (f) Corresponding visualization of the crystal structures with major planes (facets) seen in (a) and (d) indexed on the real-space unit cell. Atoms are color-coded by element: S, yellow; Ca, dusty blue; O, red; C, brown; H, beige.

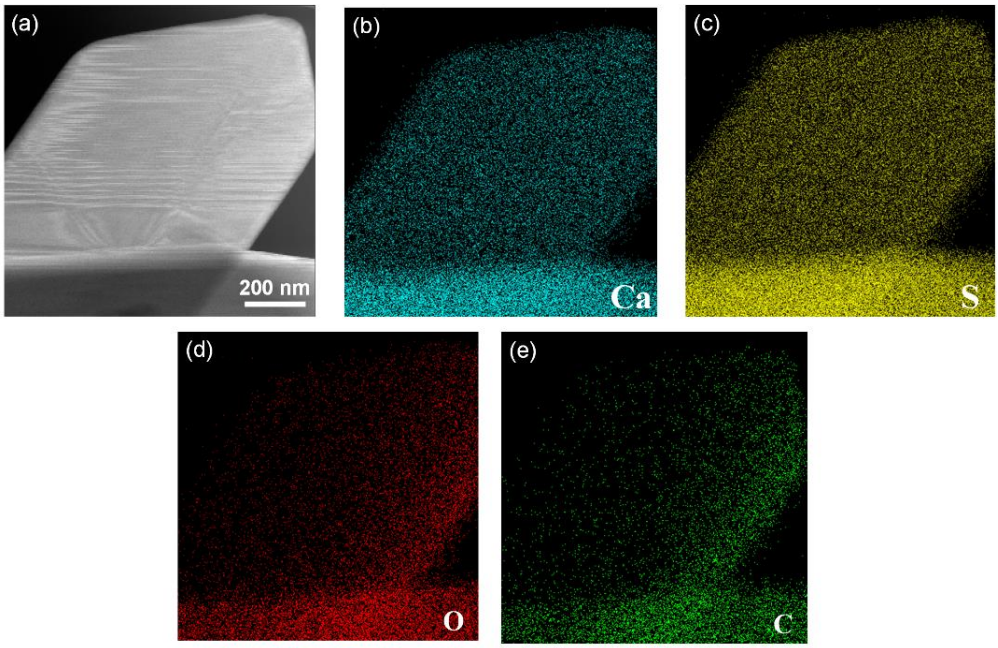

Figure S24. STEM Annular Dark Field image of Ca-NDS (water) sample, and STEM-EDS elemental maps of (b) calcium, (c) sulfur, (d) oxygen, and (e) carbon. The oxygen and carbon K_α emission occurs at low energy and is therefore affected by absorption effects within the sample, resulting in apparent inhomogeneities in the maps as a function of path from the source of X-ray emission to the X-ray detector.

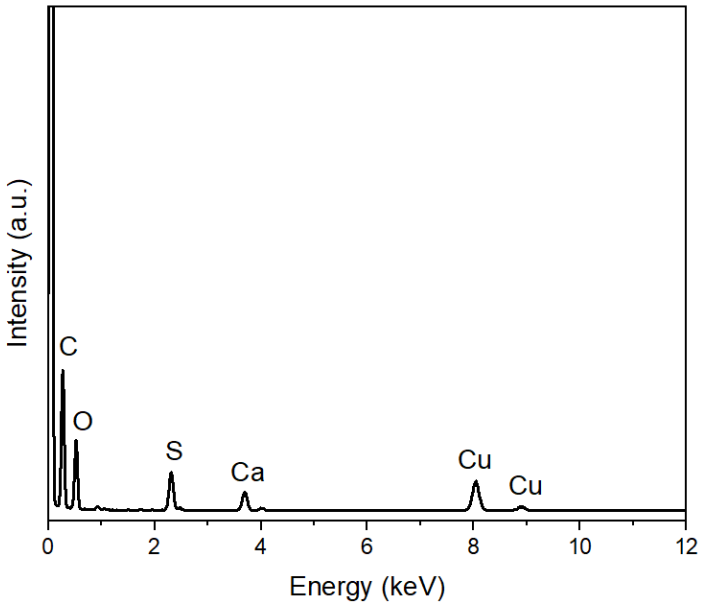

Figure S25. EDS spectra of the Ca-NDS (water) crystal shown in Figure S24.

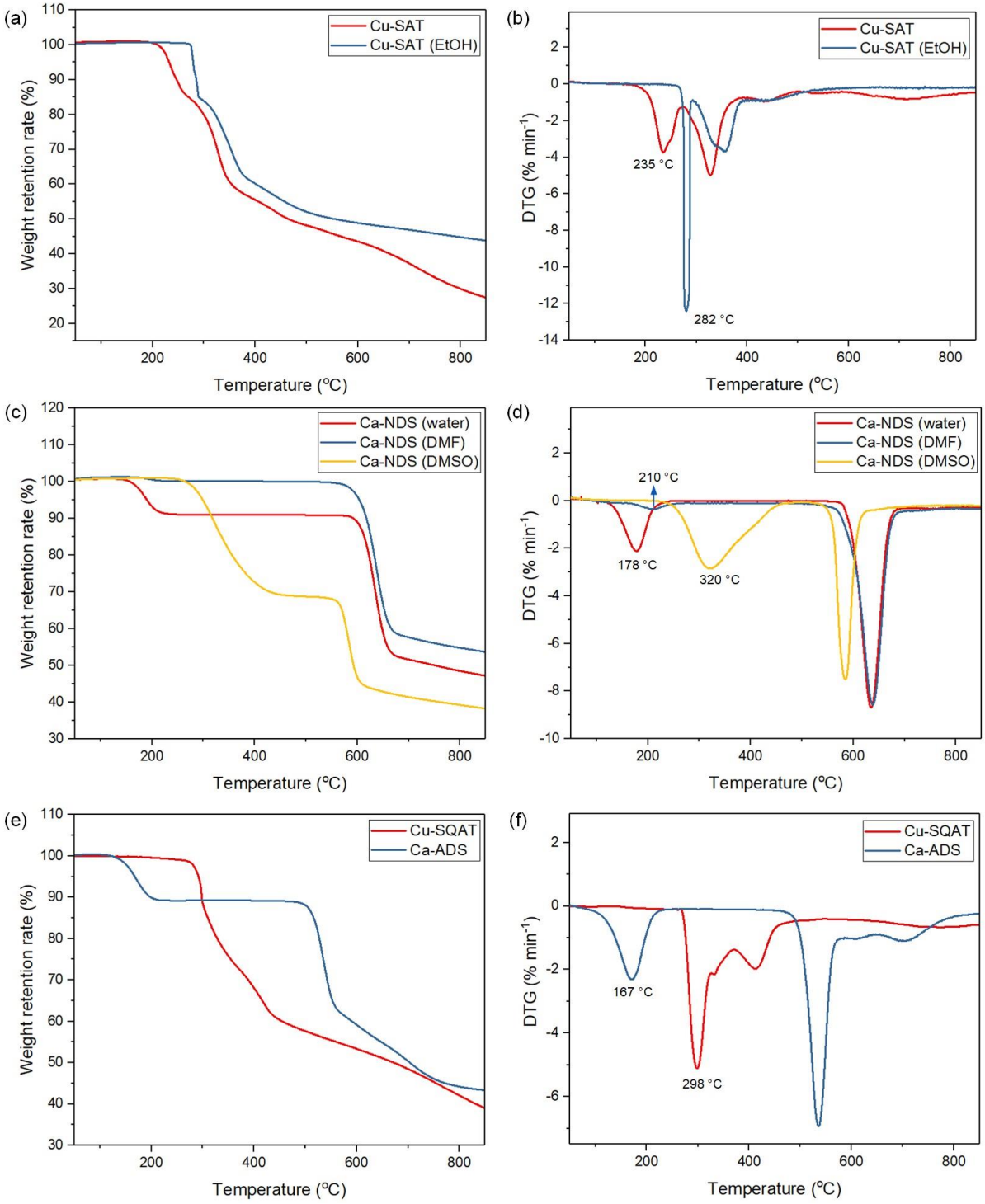

Figure S26. (a) TGA and (b) DTG results of Cu-SAT and Cu-SAT (EtOH) samples, (c) TGA and (d) DTG results of Ca-NDS (water), Ca-NDS (DMF) and Ca-NDS (DMSO) samples, and (e) TGA and (f) DTG results of Cu-SQAT and Ca-ADS samples.

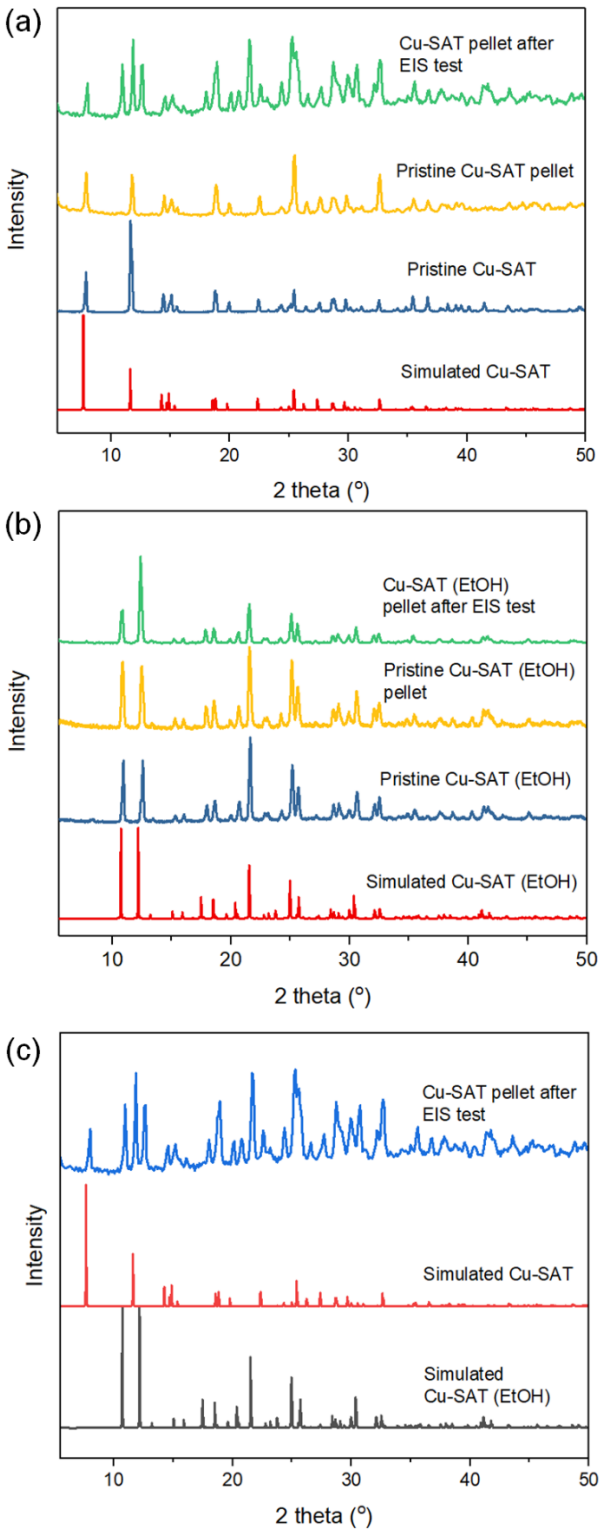

Figure S27. Experimental powder XRD patterns of (a) Cu-SAT and (b) Cu-SAT (EtOH) as a powder collected from synthesis (pristine), after pellet formation, and after EIS testing compared to powder XRD patterns simulated from the respective single crystal structures. (c) XRD patterns of Cu-SAT after EIS testing compared to powder XRD patterns simulated from Cu-SAT and Cu-SAT (EtOH).

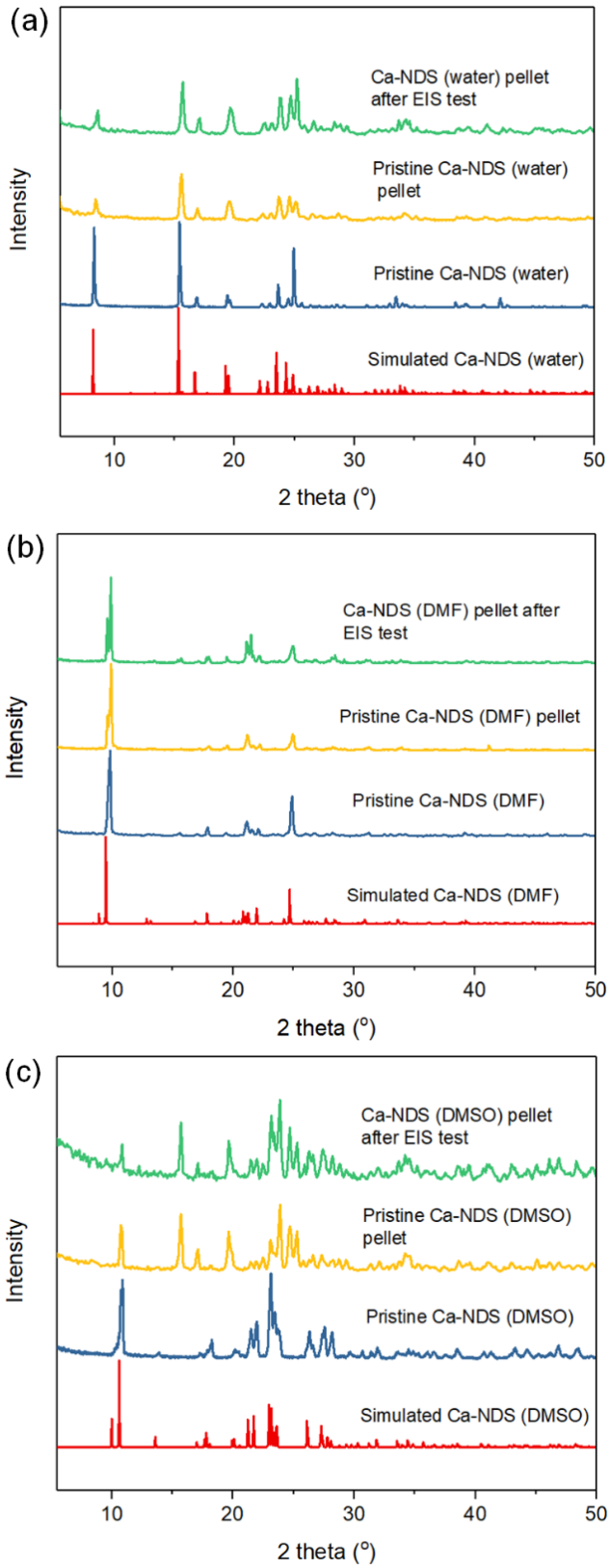

Figure S28. Experimental powder XRD patterns of (a) Ca-NDS (water), (b) Ca-NDS (DMF) and (c) Ca-NDS (DMSO) as a powder collected from synthesis (pristine), after pellet formation, and after EIS testing compared to powder XRD patterns simulated from the respective single crystal structures.

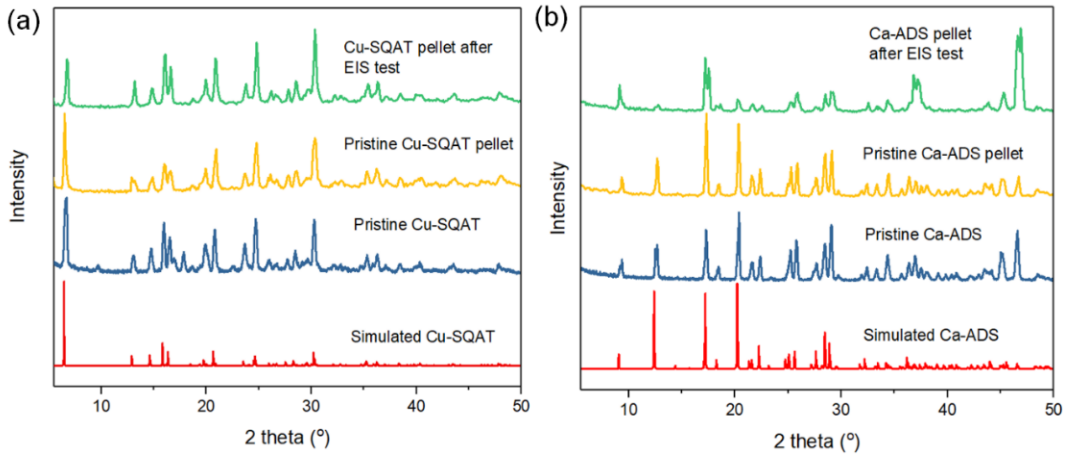

Figure S29. Experimental powder XRD patterns of (a) Cu-SQAT and (b) Ca-ADS as a powder collected from synthesis (pristine), after pellet formation, and after EIS testing compared to powder XRD patterns simulated from the respective single crystal structures.

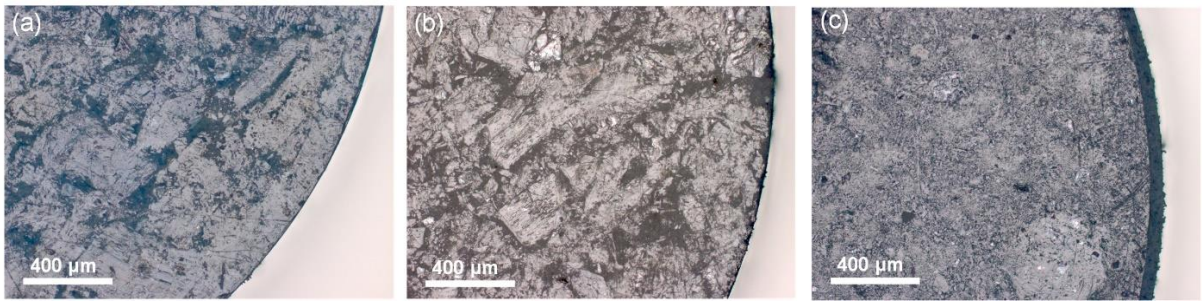

Figure S30. Light microscope images of (a) Cu-SAT, (b) Ca-NDS (water) and (c) Cu-SQAT pellets.

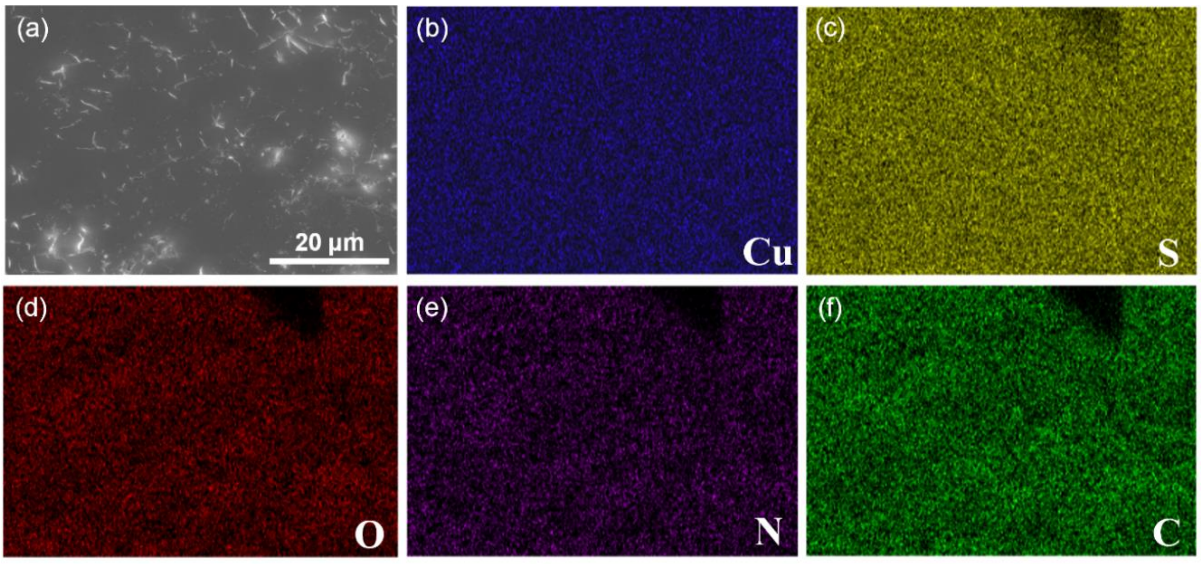

Figure S31. (a) SEM image of the Cu-SAT pellet, and SEM-EDS elemental maps of (b) copper, (c) sulfur, (d) oxygen, (e) nitrogen, and (f) carbon.

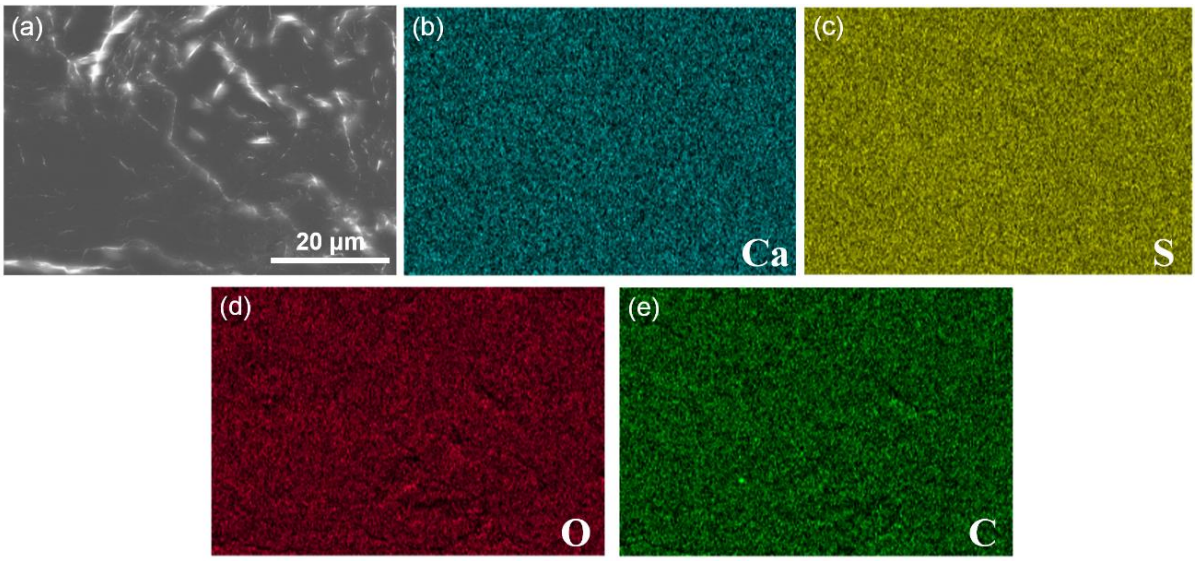

Figure S32. (a) SEM image of the Ca-NDS (water) pellet, and SEM-EDS elemental maps of (b) calcium, (c) sulfur, (d) oxygen, and (e) carbon.

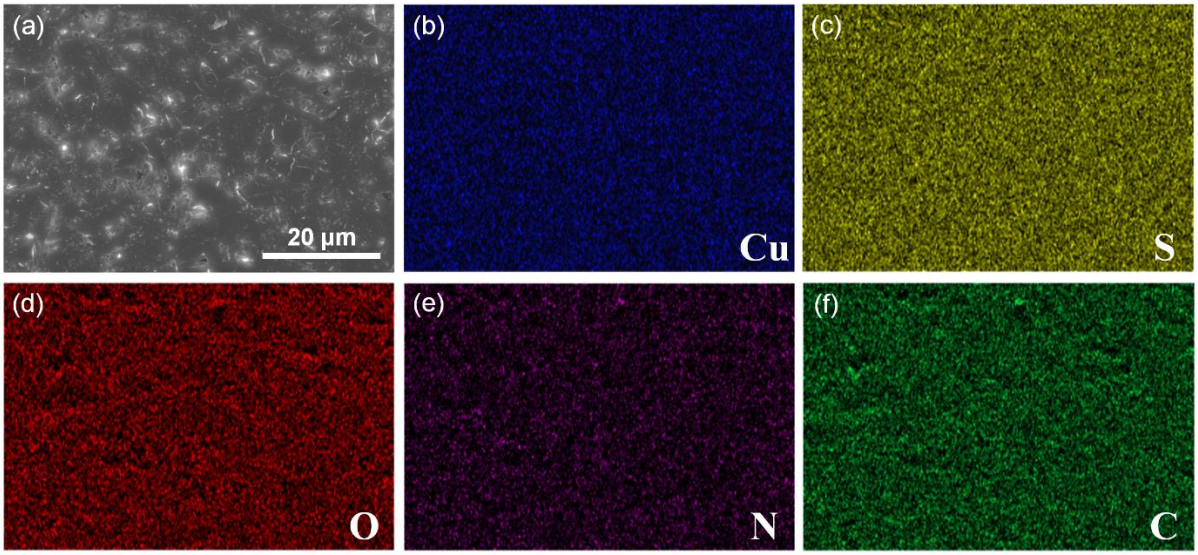

Figure S33. (a) SEM image of the Cu-SQAT pellet, and SEM-EDS elemental maps of (b) copper, (c) sulfur, (d) oxygen, (e) nitrogen, and (f) carbon.

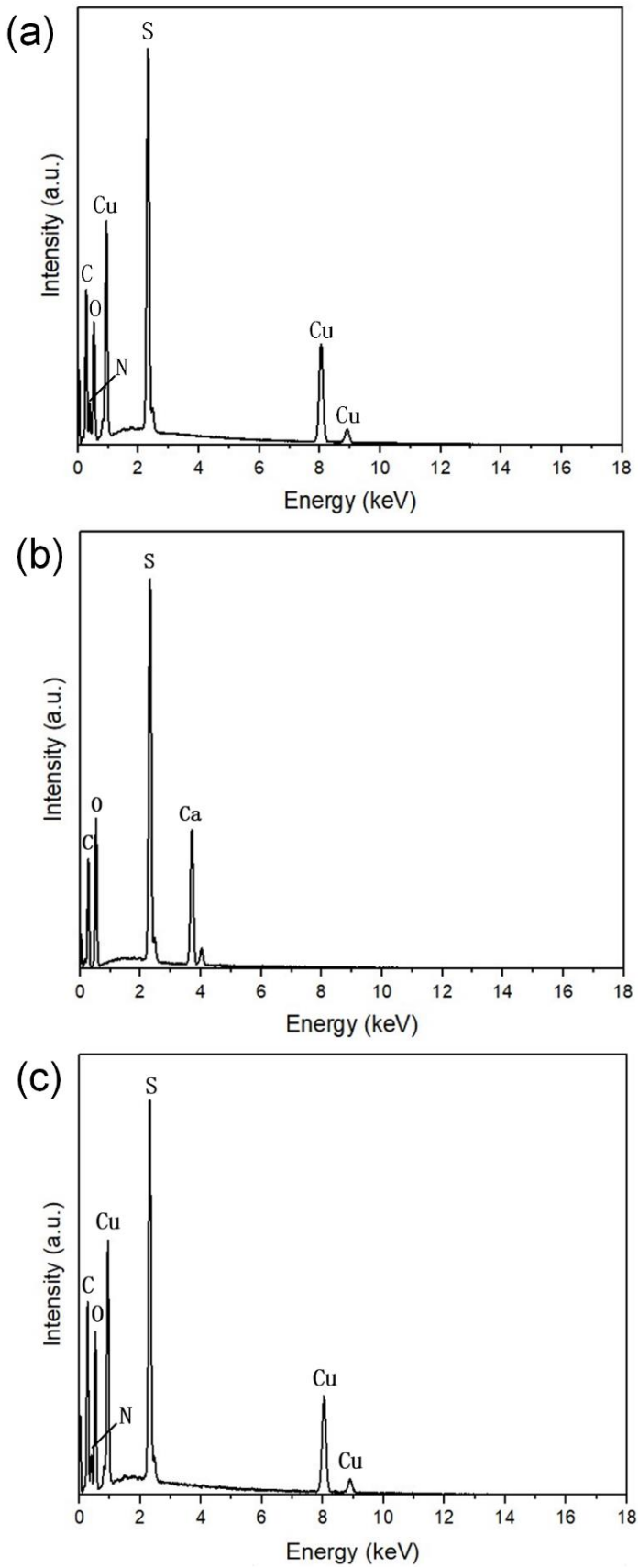

Figure S34. EDS spectra of (a) Cu-SAT, (b) Ca-NDS (water) and (c) Cu-SQAT pellets shown in Figure S31, S32, and S33, respectively.

Table S8. Density, resistance, and proton conductivities of Cu-SAT and Cu-SAT (EtOH) pellets. Uncertainties are given as one standard deviation.

Sample name	Density ($g\ cm^{-3}$)	Calculated density ($g\ cm^{-3}$)	Density as % of calculated density	Thickness (cm)	Resistance (ohm)	Proton conductivity ($mS\ cm^{-1}$)
Cu-SAT a	1.708	1.899	89.94	0.104	230	2.31
Cu-SAT b	1.719		90.52	0.094	215	2.23
AVG of Cu-SAT	1.714 ± 0.008		90.23 ± 0.41	--	--	2.27 ± 0.06
Cu-SAT (EtOH) a	1.781	2.091	85.17	0.126	1950	0.33
Cu-SAT (EtOH) b	1.798		85.99	0.092	1269	0.37
AVG of Cu-SAT (EtOH)	1.790 ± 0.012		85.58 ± 0.57	--	--	0.35 ± 0.03

Note: Density as % of calculated density is the ratio of measured density to the calculated density of crystals from the SC-XRD (ρ_{calc}/$g\ cm^{-3}$), then times 100. Resistance and proton conductivity were measured at 80 °C in 95 % RH.

Table S9. Density, resistance, and proton conductivities of Ca-NDS (water), Ca-NDS (DMF) and Ca-NDS (DMSO) pellets. Uncertainties are given as one standard deviation.

Sample name	Density ($g\ cm^{-3}$)	Calculated density ($g\ cm^{-3}$)	Density as % of calculated density	Thickness (cm)	Resistance (ohm)	Proton conductivity ($mS\ cm^{-1}$)
Ca-NDS (water) a	1.408	1.746	80.64	0.127	430	1.51
Ca-NDS (water) b	1.353		77.49	0.132	480	1.40
AVG of Ca-NDS (water)	1.381 ± 0.039		79.07 ± 2.22	--	--	1.46 ± 0.08
Ca-NDS (DMF) a	1.296	1.532	84.60	0.124	1750	0.36
Ca-NDS (DMF) b	1.332		86.95	0.110	1431	0.39
AVG of Ca-NDS (DMF)	1.314 ± 0.025		85.77 ± 1.66	--	--	0.38 ± 0.02
Ca-NDS (DMSO) a	1.449	1.703	85.09	0.127	900	0.72
Ca-NDS (DMSO) b	1.424		83.62	0.133	1030	0.66
AVG of Ca-NDS (DMSO)	1.437 ± 0.012		84.35 ± 1.04	--	--	0.69 ± 0.04

Note: Density as % of calculated density is the ratio of measured density to the calculated density of crystals from the SC-XRD (ρ_{calc}/$g\ cm^{-3}$), then times 100. Resistance and proton conductivity were measured at 80 °C in 95 % RH.

Table S10. Density, resistance, and proton conductivities of Cu-SQAT and Ca-ADS pellets. Uncertainties are given as one standard deviation.

Sample name	Density ($g\ cm^{-3}$)	Calculated density ($g\ cm^{-3}$)	Density as % of calculated density	Thickness (cm)	Resistance (ohm)	Proton conductivity ($mS\ cm^{-1}$)
Cu-SQAT a	1.702	2.066	82.38	0.117	510	1.17
Cu-SQAT b	1.751		84.75	0.093	460	1.03
AVG of Cu-SQAT	1.727 ± 0.035		83.57 ± 1.68	--	--	1.11 ± 0.09
Ca-ADS a	1.699	1.910	88.95	0.110	1300	0.43
Ca-ADS b	1.731		90.63	0.102	1130	0.46
AVG of Ca-ADS	1.715 ± 0.023		89.79 ± 1.18	--	--	0.45 ± 0.02

Note: Density as % of calculated density is the ratio of measured density to the calculated density of crystals from the SC-XRD (ρ_{calc}/$g\ cm^{-3}$), then times 100. Resistance and proton conductivity were measured at 80 °C in 95 % RH.

Table S11. Proton conductivity and synthesis condition of CPs reported in this work compared with recent references.

Sample name	Proton conductivity ($mS\ cm^{-1}$)	Synthesis condition	References
Cu-SAT	2.27 (80 °C, 95% RH)	80 °C for 3h	This work
Ca-NDS (water)	1.46 (80 °C, 95% RH)	80 °C for 3h	This work
Cu-SQAT	1.11 (80 °C, 95% RH)	80 °C for 3h	This work
MIL-68-In-OH	1.72 (100 °C, 98% RH)	125 °C for 5h	S-1
Tb-MOF	0.54 (100 °C, 98% RH)	95 °C for 72h	S-2
Sm-MOF	1.28 (100 °C, 98% RH)	95 °C for 72h	S-2
JUK-13- SO_3H-SO_2	0.23 (75 °C, 60% RH)	80 °C for 7 days	S-3
$[Cd(H_2BBT)_2]_n$	0.18 (100 °C, 98% RH)	20 °C for 7 days	S-4
$\{[Ni(p\text{-}IPhH_2IDC)_2] \cdot H_2O\}_n$	0.04 (100 °C, 98% RH)	150 °C for 96h	S-5
$[Sr(\mu_5\text{-}p\text{-}FPhHIDC)(H_2O)]_n$	0.04 (100 °C, 98% RH)	155 °C for 4 days	S-6
$[Ba(o\text{-}CPH_2IDC)]_n$	0.31 (100 °C, 98% RH)	150 °C for 96h	S-7

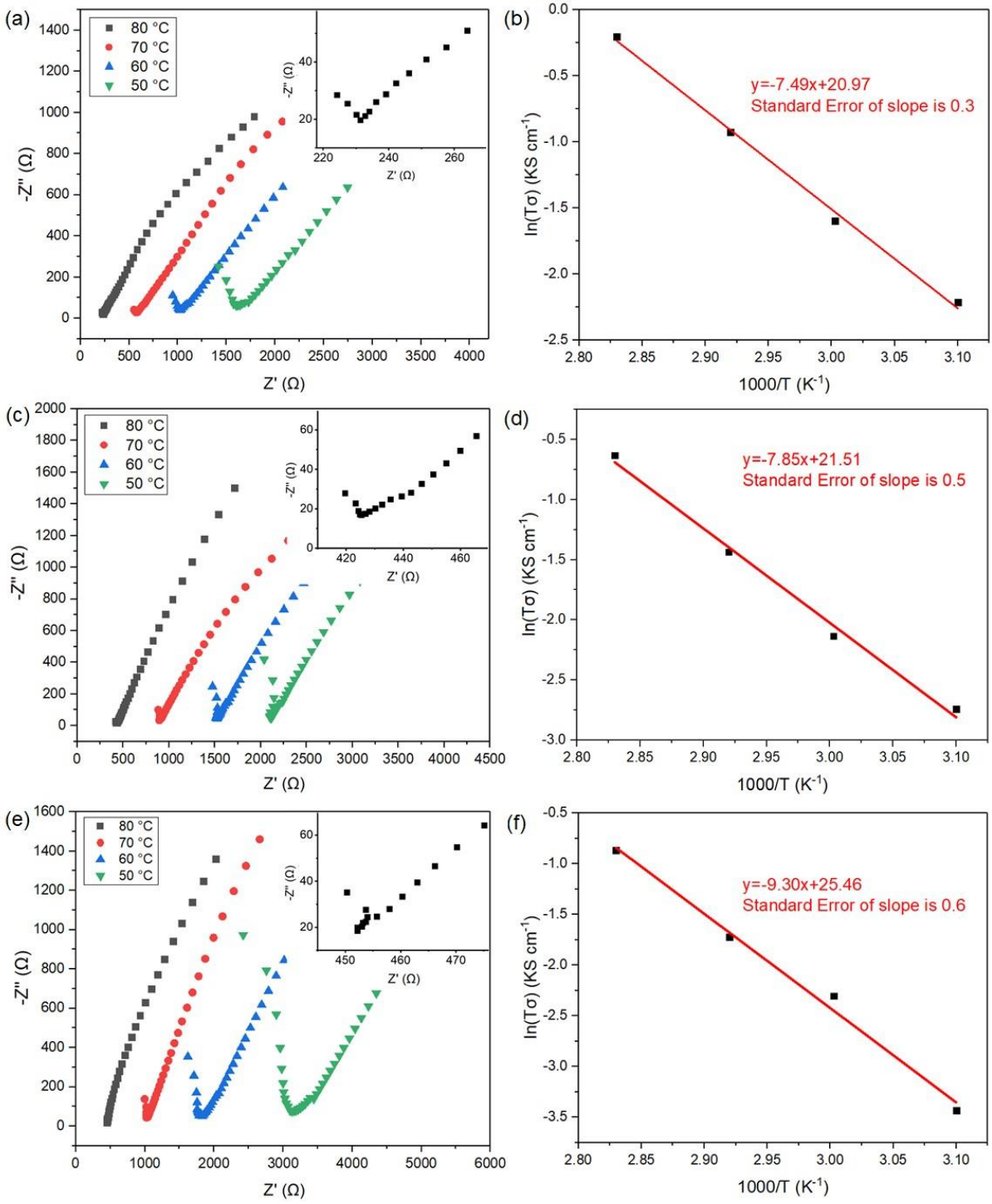

Figure S35. (a) EIS Nyquist plots and (b) Arrhenius plots of Cu-SAT pellet samples at 50-80 °C and 95% RH, (c) EIS Nyquist plots and (d) Arrhenius plots of Ca-NDS (water) pellet samples at 50-80 °C and 95% RH, (e) EIS Nyquist plots and (f) Arrhenius plots of Cu-SQAT pellet samples with temperature range 50-80 °C and 95% RH.

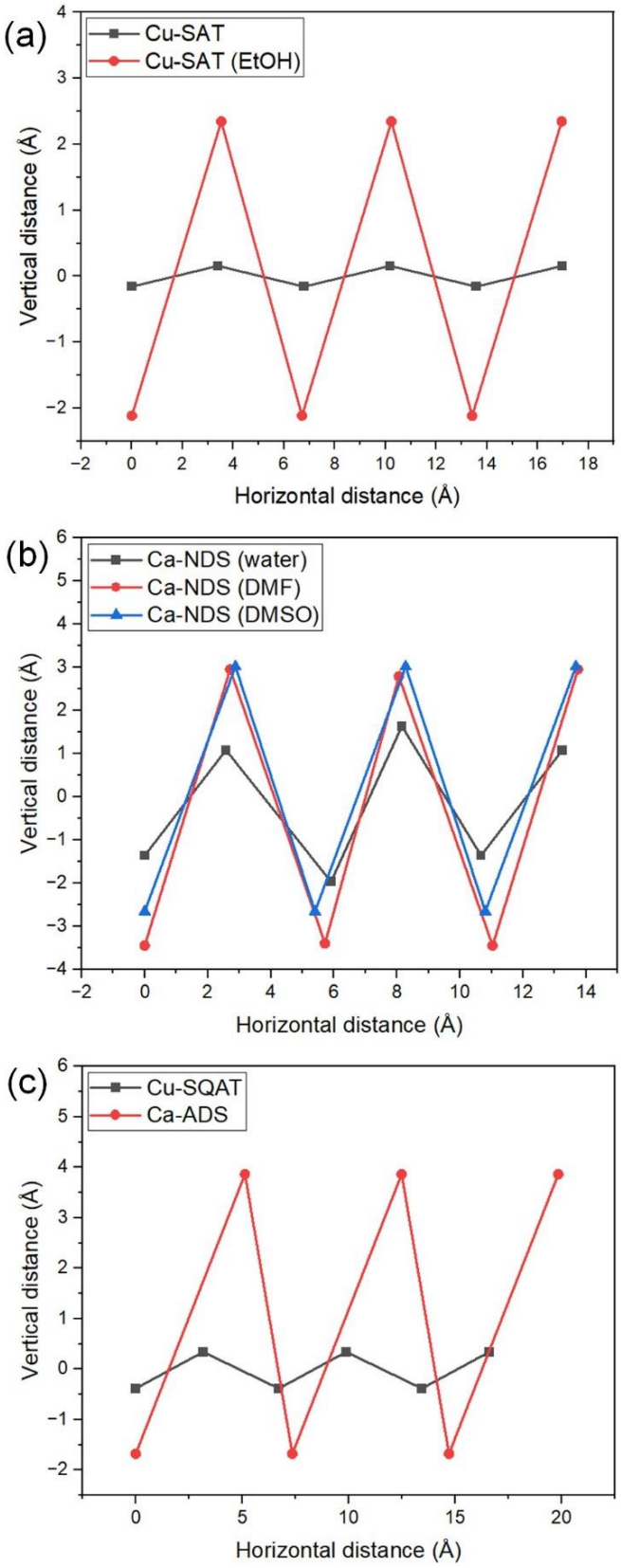

Figure S36. Distances between atoms in hydrogen bonding network chains in (a) Cu-SAT and Cu-SAT (EtOH), (b) Ca NDS samples, and (c) Cu-SQAT and Ca-ADS.

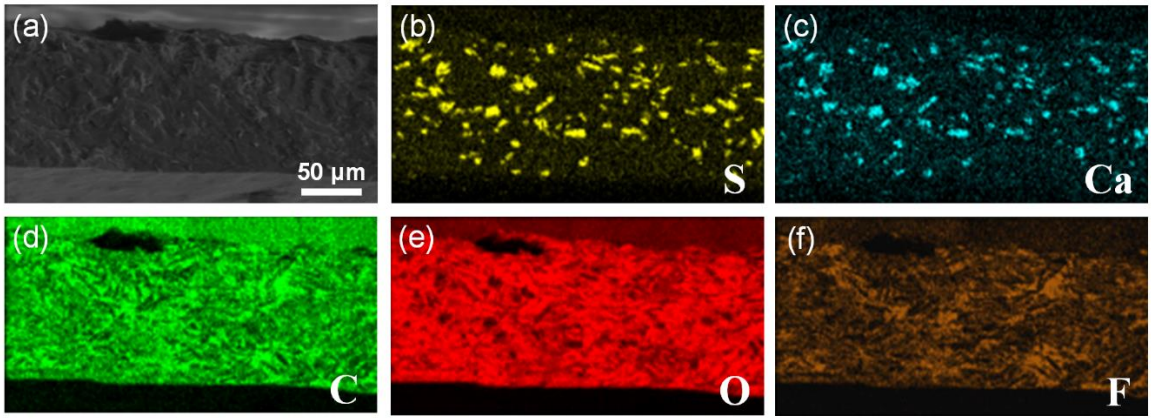

Figure S37. (a) Cryo-SEM cross-sectional image of the fully hydrated Ca-NDS (water)-MMM, and SEM-EDS elemental maps of: (b) sulfur, (c), calcium, (d) carbon, (e) oxygen, and (f) fluorine.

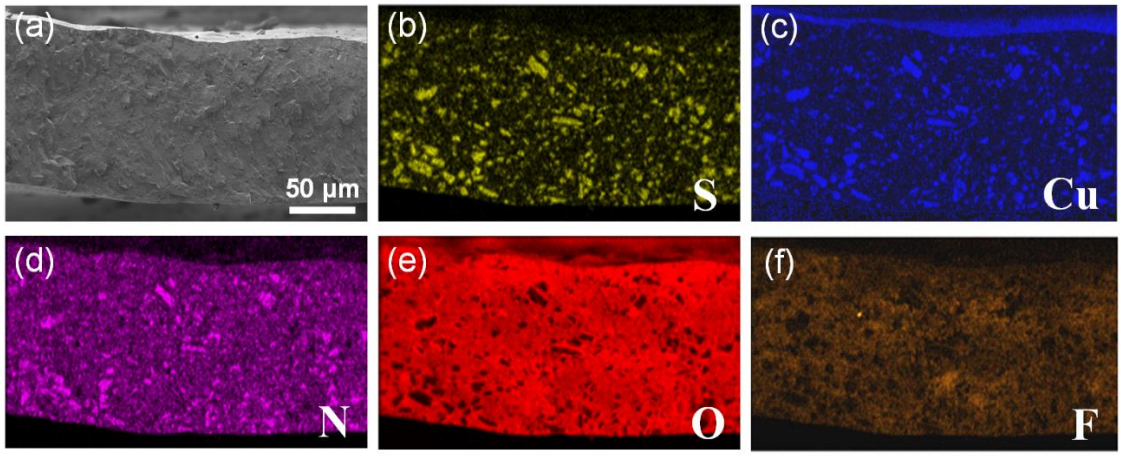

Figure S38. (a) Cryo-SEM cross-sectional image of the fully hydrated Cu-SQAT-MMM, and SEM-EDS elemental maps of: (b) sulfur, (c), cooper, (d) carbon, (e) oxygen, and (f) fluorine.

References

S-1. Y. J. Song, Y. L. Sang, K. Y. Xu, H. L. Hu, Q. Q. Zhu and G. Li, *Inorg. Chem.*, 2024, **63**, 4233-4248.
S-2. Y. L. Hong, S. W. Zuo, H. Y. Du, Z. Q. Shi, H. Hu and G. Li, *ACS Appl. Mater. Interfaces*, 2024, **16**, 13745-13755.
S-3. M. Szufla, A. Krawczuk, G. Jajko, P. Kozyra and D. Matoga, *Inorg. Chem.*, 2024, **63**, 151-162.
S-4. L. X. Xie, Z. J. Ye, X. D. Zhang and G. Li, *J. Solid State Chem.*, 2022, **311**, 123154.
S-5. H. Zhao, Z.-H. Du, C.-Y. Mu and G. Li, *J. Solid State Chem.*, 2022, **315**, 123550.
S-6. R.-L. Liu, J. Li, Y.-L. Zhao, Y.-R. Wang, X.-H. Fan, G. Li and D.-Y. Wang, *J. Solid State Chem.*, 2024, **332**, 124557.
S-7. Z. Guo, Y. Zhang, J. Liu, B. Han and G. Li, *New J. Chem.*, 2021, **45**, 16971-16977.